Summer 8-6-2019

Peroxiredoxin 6 and Phospholipids in Alzheimer's Disease

Nathan A. Drolet
Southern Methodist University, ndrolet@smu.edu

PEROXIREDOXIN 6 AND PHOSPHOLIPIDS

IN ALZHEIMER'S DISEASE

Approved by:

Prof. William Orr
Department Chair and Professor in the Biological Sciences

Prof. Richard Jones
Professor in the Biological Sciences

Prof. Svetlana Radyuk
Associate Professor in the Biological Sciences

Prof. Steven Vik
Professor in the Biological Sciences

PEROXIREDOXIN 6 AND PHOSPHOLIPIDS

IN ALZHEIMER'S DISEASE

A Thesis Presented to the Graduate Faculty of

Dedman College

Southern Methodist University

in

Partial Fulfillment of the Requirements

for the degree of

Master of Science

in

Molecular and Cellular Biology

by

Nathan Drolet

B.S., Biological Sciences, Southern Methodist University

August 6, 2019

Drolet, Nathan B.S., Biological Sciences, Southern Methodist University

Peroxiredoxin 6 and Phospholipids
In Alzheimer's Disease

Advisor: Professor William Orr
Master of Science conferred August 6, 2019
Thesis completed May 22, 2019

Although many neurological mechanisms that contribute to Alzheimer's disease (AD) have been elucidated, none so far have yielded treatments that can improve AD patient prognosis or slow progression of the disease. Oxidative stress and inflammation in the brain have been identified as major hallmarks of AD, and studies suggest these phenomena induce neurodegeneration. However, connections between AD and the development of these symptoms remain poorly understood. The redox regulator Prx6 has been implicated by studies in humans and mice as a potential mediator between these phenomena. Prx6 may be able to influence oxidative stress and inflammation simultaneously using its peroxidase (PRX) and phospholipase (PLA2) enzymatic activities, respectively. Despite these findings, the roles of each Prx6 activity in AD progression have yet to be examined.

This thesis describes a body of experiments that suggest Prx6 may indeed contribute to the severity of AD, although the current evidence is insufficient to provide conclusive proof. *Drosophila* models of AD were crossed into lines carrying genomic constructs for over- or under-expression of the two fly Prx6 homologs: dPrx2540, which has strong PRX and PLA2 active-site homology with human Prx6, and dPrx6005, which retains homology only in its PRX

site. dPrx2540 and dPrx6005 protein expression in these lines was confirmed by crosses to Gal4 driver lines and subsequent western blotting. Lifespan experiments revealed that under-expressing dPrx2540 in an amyloid-β background significantly reduces mortality. In contrast, over- or under-expression of dPrx6005 – which purportedly lacks PLA2 activity – caused significant but relatively minor changes in longevity. Additionally, locomotor tests suggest that dPrx2540 under-expression enhances activity in young and middle-aged AD flies. Recent work has focused on the creation of *Drosophila* lines in which all endogenous dPrx2540 copies are deleted using CRISPR-Cas9 methodology. These flies are being generated by designing and integrating vectors carrying Cas9 guide RNAs into the fly genome and expressing these RNAs coincidingly with germline Cas9. Mutant dPrx2540 transgenes with ablated peroxidase or phospholipase activities have also been constructed using PCR-based mutagenesis techniques. Vectors carrying these transgenes have been integrated into a separate group of flies. In the future, these flies will be combined into the dPrx2540-null background by crossing, and these CRISPR mutant dPrx2540 *Drosophila* lines will be further combined into an AD background. This will allow lifespan assays and other measurements of AD phenotypes to be performed, which will provide a more rigorous analysis of the specific roles of Prx6's two enzymatic activities in AD.

TABLE OF CONTENTS

LIST OF FIGURES

LIST OF TABLES

ACKNOWLEDGEMENTS

I owe a great deal to Dr. William Orr for his guidance throughout this project, and for helping me to mature as a scientist. I would also like to thank Dr. Johannes Bauer, who ushered me into the world of laboratory science and supported me through triumph and failure. Many members of the Orr lab, including Dr. Vladimir Klichko and Jared Ferrell-Penniman, have provided indispensable aid to the project on numerous occasions. I am also grateful for the advice of other faculty in the Biology Department who have shaped my decisions in science. Lastly, I would like to thank all of the many undergraduates who have contributed to this project over these past years, and my family, who gave me the opportunity to follow my dream.

CHAPTER 1

INTRODUCTION

1.1 Background

Alzheimer's disease (AD) is among the most debilitating neurodegenerative conditions in the world. Current estimates suggest that one in ten Americans over the age of sixty-five suffer from AD, a number that will likely grow exponentially as the US population ages (Alzheimer's Association, 2019). Psychological changes associated with AD, such as loss of complex reasoning skills and memory, are directly associated with synapse dysfunction and neurodegeneration within the cortex (Crews and Masliah, 2010). Pathological aggregates of amyloid-β and hyperphosphorylated tau are known to drive this process. But despite years of research into these proteins and other contributing factors, there is still no consensus about how neurodegeneration in AD is driven at the molecular level. Without such information, it may be impossible to discover treatments to stop it. In addition to specific proteins, many physiological processes have been shown to be disrupted by AD (Querfurth and LaFerla, 2010) . Two of these – oxidative stress and inflammation – may play a crucial role in disease progression. Individuals with AD exhibit perturbed regulation of reactive oxygen species within the brain, indicated by increased protein and lipid biomarkers of oxidation (Chen and Zhong, 2014). These oxidative species are derived largely from mitochondrial damage by amyloid-β and deliberate secretion by microglia, and they may contribute to neuron toxicity through damage to DNA and other

important biomolecules. Activated microglia are also a primary feature of AD-associated inflammation. Microglia degrade extracellular amyloid-β plaques, and are therefore in some ways beneficial in AD, but they also drive neurodegeneration through paracrine inflammatory signals and direct phagocytosis of neuronal synapses (Hansen, Hanson and Sheng, 2018). Consequently, oxidative stress and neuroinflammation are not only definite features of AD, but are also responsible for driving its progression.

Peroxiredoxin 6 (Prx6) is a member of the peroxiredoxin family, a class of antioxidant proteins that reduce cellular peroxides to maintain a healthy redox balance (Kim, Lee, and Kim, 2016). Like the rest of its family, Prx6 reduces various peroxide compounds using a catalytic cysteine in its peroxidase (PRX) active site, albeit using a 1-cysteine variation of the usual 2-cysteine mechanism. However, Prx6 also possesses an acidic calcium-independent phospholipase A2 (aiPLA2) activity via a catalytic serine with supporting histidine and aspartate residues, which allows it to cleave the sn-2 acyl bond of phospholipids in the cell membrane. This action produces arachidonic acid in many cases (Murakami and Kudo, 2002). Arachidonic acid is a major metabolic intermediate for inflammatory eicosanoids, thus contributing to inflammation. Furthermore, cytosolic PLA2 enzymes have been implicated in amyloid-β-induced neurotoxicity (Thomas, Pelleieux, Vitale, and Olivier, 2016). These observations suggest that Prx6 may be able to influence both the oxidative stress and inflammatory components of AD. In fact, postmortem studies of AD patients have revealed significantly elevated levels of Prx6 in the brain, especially in activated astrocytes localized around amyloid-β plaques (Power, Asad, Chataway, Chegini, Manavis, Temlett, Jensen, Blumbergs, and Gai, 2008). Additionally, mouse models of AD with transgenic Prx6 over-expression exhibit worse AD symptoms than their control counterparts, including increased glial activation and decreased

memory (Yun, Jin, Han, Lee, Han, Oh, Hong, Jung, and Hong, 2013). These studies suggest that Prx6 expression is upregulated in AD and contributes significantly to disease severity. However, no studies have yet determined the mechanism by which Prx6 modulates AD severity, or whether this mechanism can be therapeutically disabled to alleviate symptoms of AD.

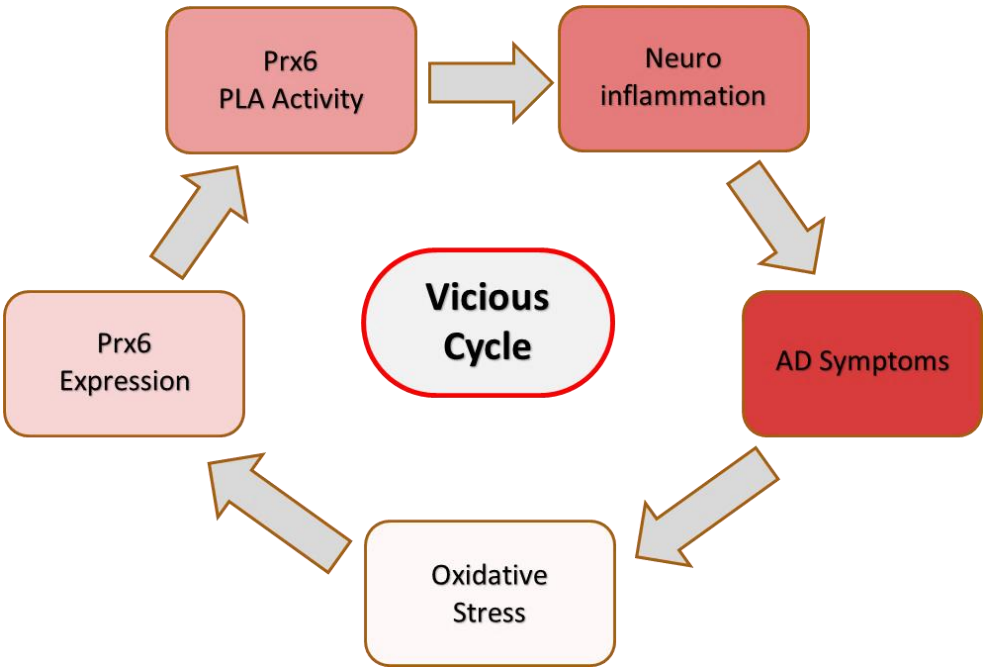

Figure 1.1 A model for Prx6 upregulation and contribution to AD. AD initiates oxidative stress, which drives Prx6 expression as a defense against reactive oxygen species. Increased Prx6 causes increased phospholipid hydrolysis and arachidonic-acid production via the Prx6 PLA2 activity, leading to neuroinflammation and further damage to neurons.

1.2 Hypothesis

Given this information, it was hypothesized that Prx6 accelerates the progression of AD severity using its PLA2 activity. Prx6 is known to be upregulated in response to oxidative stress

in some circumstances (Chowdhury, Mo, Gao, Kazi, Fisher, and Feinstein, 2009). Consequently, Prx6 may drive a kind of 'vicious cycle' in AD, detailed in Figure 1.1. This model proposes that amyloid-β or other factors implicit to AD induce oxidative stress in the brain, which in turn causes neurons and glia to upregulate antioxidant enzymes – including Prx6 – as a compensatory response. Prx6 then liberates arachidonic acid from phospholipids in the cell membrane, starting a pathway that results in neuroinflammation and inflammation-induced neuronal damage.

Figure 1.2 Homologies between *H. sapiens* and *D. melanogaster* Prx6 orthologs. Top graphic compares protein sequence of dPrx2540-1 (Query) to human Prx6 (Subject). Bottom graphic compares sequence of dPrx6005 to human Prx6. Red boxes indicate the homologous catalytic Cys at the PRX active site, while green boxes indicate the Ser, His and Asp for PLA2 activity. Note that dPrx6005 shares the catalytic Cys and surrounding residues with Prx6, but lacks the His and Asp that are essential to the PLA2 active site. dPrx2540-1 and dPrx6005 polypeptide sequences are from UniProt database, https://www.uniprot.org/uniprot/A1Z892#sequences and https://www.uniprot.org/uniprot/Q9GPQ2. Homology search and alignment was performed with protein-protein BLAST from the U.S. National Library of Medicine, https://blast.ncbi.nlm.nih.gov/Blast.cgi.

Drosophila melanogaster possess two homologs of mammalian Prx6, called dPrx2540 and dPrx6005. dPrx2540 and dPrx6005 share about 50-60% homology with human Prx6, as shown in Figure 1.2. Crucially, dPrx2540 shares sequence homology with Prx6 at the predicted PLA2 active site, but dPrx6005 does not. This means that dPrx2540 likely shares the same PRX and PLA2 activities as human Prx6, whereas dPrx6005 lacks the PLA2 activity. Consequently, it was predicted that dPrx2540 could have a negative impact on AD in *Drosophila* due to its PLA2 activity. dPrx6005 should have little impact on AD, due to its lack of PLA2 activity, or it may even improve AD symptoms because its PRX activity can reduce the ROS burden in the brain.

1.3 Objectives

Two experimental aims were devised to test whether the PLA2 activity of Prx6 is responsible for its impact on AD, using *Drosophila* models of the disease. The first aim examines whether *Drosophila*'s bifunctional Prx6 homolog (dPrx2540) or its monofunctional homolog (dPrx6005) impact AD phenotypes when over- or under-expressed in AD flies:

1. Create lines with concurrent expression of amyloid-β and over- or under-expression of dPrx2540 or dPrx6005 (hereafter called AD-dPrx lines), expressed via Gal4-UAS system.
2. Confirm dPrx expression levels in the AD-dPrx lines by Western blot.
3. Test AD-dPrx lines for changes in health parameters that are afflicted in AD:
    - Lifespan, measured by counting daily mortality and calculating statistical differences in survivorship between lines.

- Locomotor activity, measured by counting the times flies cross up and down a vial each day, which approximates overall activity levels for each line.

4. Additionally, test for the effects of PLA2 inactivation in AD-dPrx flies, using chemical inhibitors of PLA2 activity.

The second aim studies the independent effects of dPrx2540's PRX and PLA2 activities on AD phenotypes in *Drosophila*:

1. Delete endogenous dPrx2540 isoforms from the *Drosophila* genome using CRISPR-Cas9. Flies possess three copies of dPrx2540 (dPrx2540-1, dPrx2540-2 and dPrx2540-3), so multiple independent Cas9 deletion steps must be performed.
2. Create mutant alleles of dPrx2540 with ablated PRX or PLA2 active sites.
3. Integrate mutant and wild-type dPrx2540 alleles into the dPrx2540-null line.
4. Perform similar lifespan and locomotor tests as described in the first aim, to determine whether mutation of the PLA2 or PRX active sites has a crucial impact on the ability of dPrx2540 to modulate AD severity in *Drosophila*.

All objectives in the first aim have been reached, except for a second lifespan assay and three PLA2 inhibitor tests that are currently underway. For aim two, dPrx2540-2 has been deleted and dPrx2540 constructs with ablated PRX or PLA2 active sites have been generated, but deletion of dPrx2540-1 and dPrx2540-3 is still in progress.

CHAPTER 2

METHODS

2.1 *Drosophila* AD and dPrx Lines

The two primary *Drosophila* AD lines used in this project – hereafter designated Aβ33773 and Aβ33774 – were acquired from the Bloomington Drosophila Stock Center (designated "BDSC: 33773" and "BDSC: 33774" in FlyBase). A similar AD line, Aβ159, was created by the Crowther lab at the University of Cambridge. All three of these lines have a P-element that carries part of the coding sequence for human amyloid precursor protein (APP) corresponding to residues 1-42. This construct is integrated into chromosome 2 for lines Aβ33773 and Aβ159, and into chromosome 3 for Aβ33774. The expressed protein comprises residues 1-42 of APP, equivalent to the cleaved form of amyloid-β found predominantly in AD, with a fused *argos* or *necrotic* extracellular secretion signal. This transgene also possesses a glutamine-to-glycine "Arctic" mutation associated with a strong familial form of AD in humans (Nilsberth, Westlind-Danielsson, Eckman, Condron, Axelman, Forsell, Stenh, Luthman, Teplow, Younkin, Näslund, and Lannfelt, 2001). Previous research has demonstrated that expression of amyloid-β in *Drosophila* – including the Arctic variant – causes symptoms like those seen in human AD patients, including neurodegeneration, extracellular amyloid-β aggregates, lifespan deficits and locomotor dysfunction (Crowther, Kinghorn, Miranda, Page, Curry, Duthie, Gubb, and Lomas, 2005), as well as learning and memory loss (Iijima, Liu, Chiang, Hearn, Konsolaki,

and Zhong, 2004). Many Drosophila AD models have been generated using amyloid-β, as well as tau-based models (Iijima-Ando and Iijima, 2010) *Drosophila* lines with genetic constructs for over- or under-expression of the Prx6 homologs dPrx2540 or dPrx6005 were created previously in this lab, and their genomic integration was previously confirmed by PCR. Over-expressor constructs contain the cDNA sequence of dPrx2540 or dPrx6005 inserted at the Multiple Cloning Site of vector pUASTattB, shown in Figure 2.1. These constructs were integrated into the *Drosophila* genome at the attP40 site on chromosome 2, utilizing ΦC31 recombinase to mediate recombination with attB sites (Bischof, Maeda, Hediger, Karch, and Basler, 2007). Over-expressor constructs are hereafter denoted as UAS-Prx2540 and UAS-Prx6005. Each under-expressor construct contains two copies of a short dPrx2540 or dPrx6005 cDNA sequence inserted on either side of a small intron, in opposite orientations, creating an siRNA hairpin when transcribed. These siRNAs were inserted into a pWIZ vector, shown in Figure 2.2, and were integrated into the *Drosophila* genome by P-element transformation. Under-expressor constructs are hereafter denoted as RNAi-Prx2540 and RNAi-Prx6005.

The amyloid-β transgenes, dPrx over-expressor transgenes, and dPrx siRNAs all utilize UAS elements in their promoters, which require the yeast-derived transcription factor Gal4 to activate transcription. Because expression of Gal4 is controlled by its own promoter, which is taken from an endogenous *Drosophila* gene, this permits control over the timing and tissue-specific expression of any UAS-regulated genes in the fly (Jeibmann and Paulus, 2009). Two major Gal4 lines (referred to as 'driver lines') were used in this project: "Da" expresses Gal4 under the control of the promoter from Daughterless, providing strong global expression, whereas "ELAV" uses the Embryonic Lethal Abnormal Vision promoter and consequently only expresses its target genes in neuronal cells. Other drivers used in this project include "Tub"

(Tubulin) for strong global expression, “Arm” (Armadillo) for weak global expression, and “APPL” (Amyloid Precursor Protein-Like) for weak neuronal expression. All amyloid-β and dPrx lines used to generate AD-dPrx flies were previously backcrossed into the reference *yw* strain for at least ten generations.

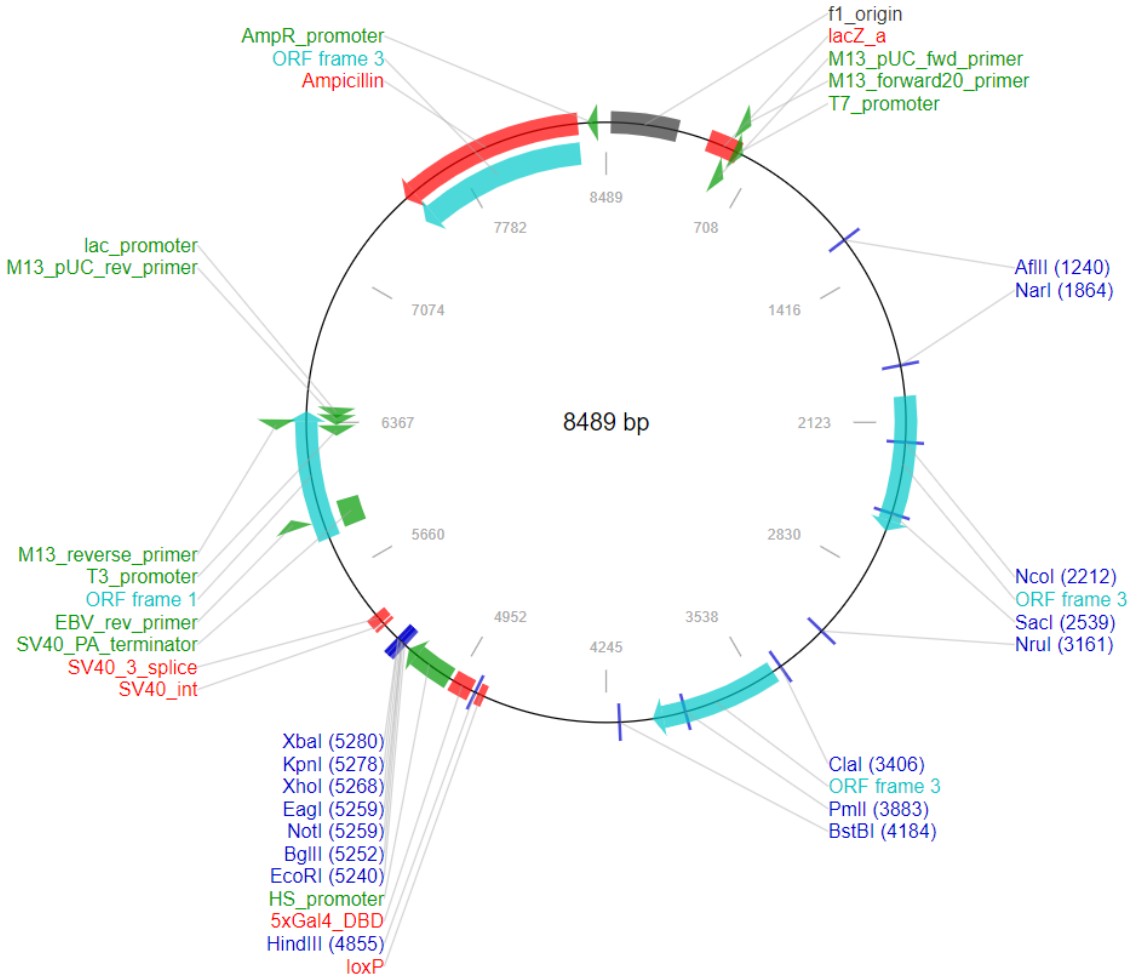

Figure 2.1 pUASTattB structure. dPrx2540 and dPrx6005 over-expressor lines possess genome-integrated pUASTattB with dPrx2540 or dPrx6005 cDNA inserted between the BglII and XhoI restriction sites. The inserted gene is expressed under the control of an hsp70 promoter and five UAS sequences (5xGal4_DBD). From Addgene, https://www.addgene.org/vector-database/5556/.

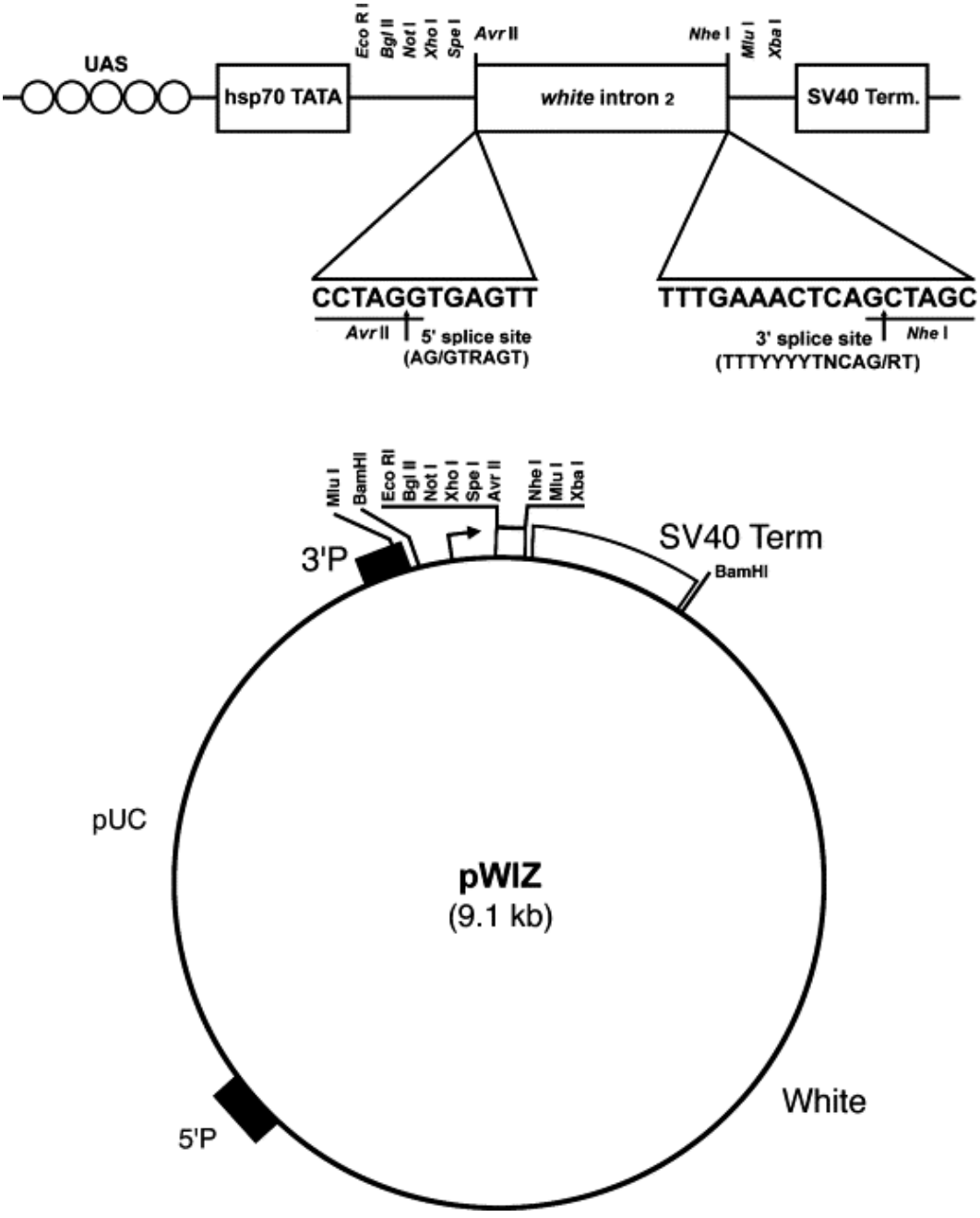

Figure 2.2 pWIZ structure. siRNA genes for dPrx2540 and dPrx6005 under-expression were created by inserting a short cDNA sequence complementary to the dPrx mRNA into the cloning sites at each end of *white* intron 2, shown at top (Lee and Carthew, 2003). The resulting siRNA is transcribed under the control of UAS elements.

Table 2.1 lists abbreviations used in this paper to indicate what combination of Gal4-driver, amyloid-β construct, and/or dPrx construct are present in a particular fly group.

Abbreviation	Genotype
X/+	Has Gal4 driver X (Da-Gal4 or ELAV-Gal4).
X > AB	Has Gal4 driver X and a UAS-regulated amyloid-β construct (Aβ33773 or Aβ33774).
X > RNAi-PrxY	Has Gal4 driver X and a UAS-regulated siRNA construct for knockdown of dPrxY (dPrx2540 or dPrx6005).
X > UAS-PrxY	Has Gal4 driver X and a UAS-regulated construct for over-expression of dPrxY.
(X > RNAi-PrxY + AB) or (X > UAS-PrxY + AB)	Has Gal4 driver X, a UAS-regulated construct for knockdown or over-expression of dPrxY, and a UAS-regulated amyloid-β construct.
(+/RNAi-PrxY + AB) or (+/UAS-PrxY + AB)	Has a UAS-regulated construct for knockdown or over-expression of dPrxY, and a UAS-regulated amyloid-β construct, but no Gal4 driver.

Table 2.1 *Drosophila* genotype abbreviations used in this paper.

2.2 Generation of Multi-Construct Lines

Double-transgenic *Drosophila* lines containing both amyloid-β and a UAS-Prx or RNAi-Prx construct for dPrx2540 or dPrx6005 were generated by crossing two of these mono-transgenic lines in a multistep process. If the constructs were on separate chromosomes, each construct line was crossed to flies with two balancer chromosomes, which confer screenable phenotypes and prevent recombination. If the constructs were on the same chromosome, meiotic

recombination was required to generate stable homozygous lines with both constructs. dPrx2540 over-expressors and ELAV-Gal4 or APPL- Gal4 neuronal driver lines were also crossed to create lines with homozygous copies of the driver and UAS-dPrx2540. Schemes for these crosses are provided in Figure 2.3. Crosses have also been made to establish lines with homozygous ELAV-Gal4, dPrx2540 over-expression, and an amyloid-β construct; however, the first attempt at this crossing scheme failed, and a second attempt is still in progress.

2.3 Experimental-to-Driver Crosses for Analysis

AD-dPrx and single-construct control lines without ELAV or APPL had to be crossed to driver lines to drive expression of their UAS-regulated constructs. Male flies with amyloid-β, a UAS-Prx construct and/or an RNAi-Prx construct were raised in standard agar food bottles with 10 ml/L tetracycline, to eliminate pathogens that could be transmitted to future generations. Female flies with Da-Gal4 or ELAV-Gal4 were similarly raised. Offspring of these males and females were crossed in standard agar food bottles without tetracycline. Each AD-dPrx was also crossed to *yellow-white* (hereafter *yw*) flies to control for any insertional effects caused by the position of the constructs. Offspring of these crosses possessed a heterozygous copy of every UAS-regulated construct carried by the male parent, and a heterozygous copy of the Gal4-driver gene carried by the female parent. These offspring were passed into fresh bottles within 48 hours of eclosion, then collected into vials with standard agar food. All cross bottles and offspring vials were kept at 28^{o}C unless otherwise noted, which contracts fly lifespan relative to colder temperatures (Miquel, Lundgren, Bensch, and Atlan, 1976).

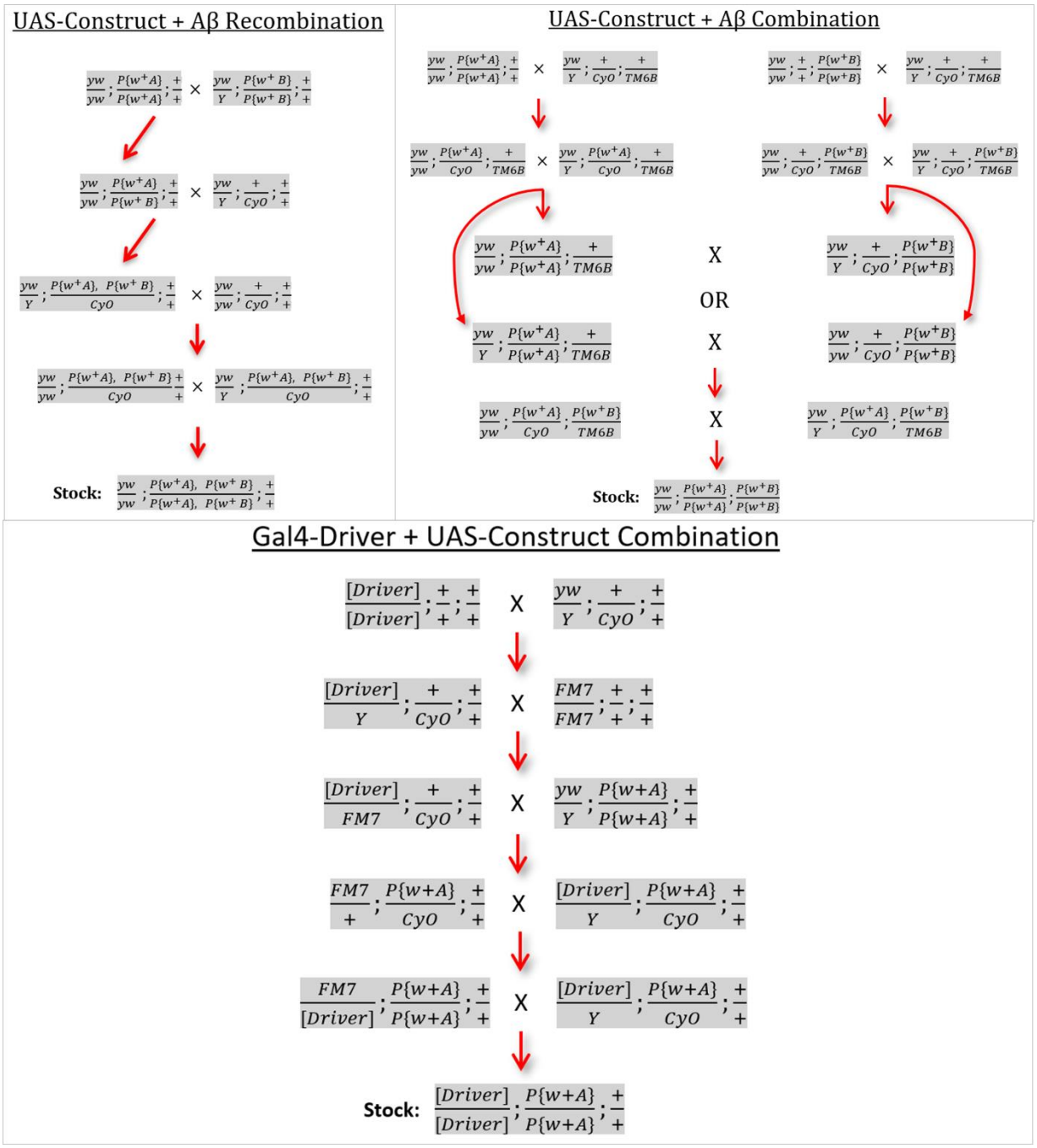

Figure 2.3 Crossing schemes for combining transgenic constructs. Gray boxes represent specific fly genotypes. Symbols above and below the horizontal lines in each box represent sister chromosomes: first line indicates sex chromosomes, second line chromosome 2, and third line chromosome 3. Letters denote chromosome properties, such as mutations in the yellow and white genes in the *yw* X chromosome. P{w$^+$A} and P{w$^+$B} are amyloid-β or dPrx constructs. CyO, TM6B and FM7 are balancer chromosomes, which block recombination and give flies specific phenotypes. 'x' indicates a cross between two genotypes. Arrows point to offspring of the previous cross, or to the 'x' if both flies in a cross are offspring of the previous cross.

2.4 Protein Isolation and Western Blotting

For AD-dPrx lines and single-construct controls, protein was isolated from the offspring of crosses between the experimental or control lines and specific driver lines, as described in Methods section 2.3. Homozygous driver-expressor flies were collected directly without extra crossing. For whole-fly protein measurements, around 10-20 flies were collected in 1.7 mL microtubes and homogenized in lysis buffer with added EDTA and protease inhibitors, 10 μL per fly. Homogenates were centrifuged to pellet insoluble material, and the supernatant was transferred to fresh tubes. Supernatants were then combined with an equal volume of dye containing β-mercaptoethanol and boiled for at least 3 minutes. Total protein concentrations were measured by Lowry assay using a UV-1800 spectrophotometer (Shimadzu). For head protein measurements, around 50-100 offspring from each cross were collected in 15 mL Eppendorf tubes. These tubes were then dipped in liquid nitrogen and vortexed briefly, which separates the heads from their thoraces. The resulting fly parts were sifted through 0.71 mm and 0.50 mm sieves, and heads were collected from the 0.5 mm sieve and transferred to microtubes. All subsequent isolation steps were the same as for whole flies.

Western blots were prepared by running protein samples through 13% polyacrylamide gels and transferring to nitrocellulose membranes by electrophoresis. Membranes were stained with Ponceau dye and imaged prior to antibody incubations. Rabbit anti-dPrx2540 and anti-dPrx6005 primary antibodies were used to bind dPrx2540 and dPrx6005, as well as mouse anti-actin primary antibodies in the same incubation. HRP-conjugated anti-rabbit and anti-mouse were used in secondary incubation. Membranes were washed in phosphate-buffered saline to remove excess antibodies, then incubated 5 minutes with ECL Western Blot Prime Detection reagents (Genesee Scientific) and imaged for chemiluminescence using Bio-Rad ChemiDoc MP

Imaging System. dPrx2540 and dPrx6005 band intensities were calculated using Bio-Rad Image Lab v5.2.1. Expression levels per lane were calculated relative to controls, in Microsoft Excel, after normalizing the data to actin levels to control for differences in the amount of fly material per lane. Staining intensities from the pre-antibody Ponceau incubations were also used for normalization in some cases, but were generally less reliable than actin due to greater variation in background staining.

2.5 DNA Isolation, PCR and Electrophoresis

Genomic DNA was isolated using materials and procedures from Puregene Core Kit A solid tissue protocol (Qiagen), Quick-DNA Universal kit (Zymo Research), or QuickDNA MiniPrep Plus kit (Zymo Research). Samples included 5-50 flies each, depending on the experiment, and were homogenized similarly to protein samples used for western blotting. Plasmid DNA was isolated from bacterial liquid cultures using materials and procedures from Qiagen Plasmid Mini, Midi, or Maxi kit, depending on the mass of DNA required for future experiments. DNA concentrations were calculated from sample absorptions at 260 and 280 nm, using a UV-1800 spectrophotometer (Shimadzu).

Non-quantitative PCR experiments were conducted with GoTaq Hot Start Master Mix (Promega), 0.5 μM forward and reverse primers, and nuclease-free water. For PCR products used in vector construction, high-fidelity Q5 High-Fidelity 2X Master Mix (New England Biolabs) was used in place of Hot Start, to lower the chance of random mutations during DNA amplification. Conventional PCR was carried out in a Mastercycler Personal (Eppendorf) thermal cycler, typically with 32 cycles of annealing, elongation and denaturation. Annealing

temperatures and elongation time were adjusted depending on primer melting temperatures and the expected PCR product length.

Electrophoresis of PCR products were performed using 1.4% agarose gels, with roughly 10 ng/ml ethidium bromide. Gels were electrophoresed at 100 volts in 0.5X TAE buffer, with extra ethidium bromide added to the TAE to enhance band intensities. Gel images were acquired using Bio-Rad ChemiDoc MP Imaging System. DNA molecular weight ladders were run in every gel to identify bands by size.

2.6 RNA Isolation and Quantitative PCR

RNA was isolated from driver-expressor flies using TRIzol Reagent protocol (Ambion, Inc.) or Direct-zol RNA Miniprep Plus kit (Zymo Research). Optional DNase-I treatment was applied in some cases with the Direct-zol kit, but had no apparent impact on RNA yield or purity. RNA samples were reverse-transcribed into cDNA using MMLV reverse transcriptase, RNAsin, 40 mM dNTPs, and MMLV 5X buffer (all Promega), or using Maxima H Minus cDNA Synthesis Master Mix with DNase (ThermoFisher). Oligo-deoxythymidine oligonucleotides were added as primers to bind mRNA poly-A tails. In some cases, gene-specific primers were used rather than oligo-dT, to eliminate possible background signal. Non-RT control reactions were prepared by excluding MMLV from the reaction mix. Samples were incubated 1 hour at 37^{o}C, then 5 minutes at 98^{o}C to inactivate MMLV. Quantitative PCR of anti-microbial peptides (AMPs) was performed by mixing cDNA samples with GoTaq qPCR Master Mix (Promega) primers specific to each AMP, as well as primers specific to the RP49 mRNA to normalize for total mRNA quantity. Reactions were run in a Rotor-Gene 3000 thermal cycler (Corbett Research). Cycle were run at 95^{o}C for 30 seconds, 50^{o}C for 30 seconds, and 72^{o}C for 30 seconds, and a final melting phase ramping from 50^{o}C to 99^{o}C.

2.7 Lifespan Assays

Lifespan experiments were conducted on the offspring of crosses between experimental or control lines and driver lines, as described in Methods section 2.3. A total of 125 males and females were collected for each cross, with 25 flies per collection vial. Vials were kept at 28ºC with 12 hour day/night cycle. Living flies in each vial were passed to fresh food vials daily, and the number of dead flies on each day was recorded. This process continued until no living flies remained in any vials. Survivorship curves and significant differences in lifespan were generated from these data using Prism 5.0c software (GraphPad Software, Inc.). Both lifespan assays in this project were conducted under essentially identical conditions.

2.8 Locomotor Assays

Both locomotor assays were performed using offspring of the same crosses used for the dPrx2540 lifespan assays. In the first locomotor experiment, flies were transferred from the standard agar food vials to liquid-food vials prior to locomotor analysis. These vials had a small cotton wad and thin cotton plug at the bottom, 1-2 cm deep, and were soaked with a nutritional liquid media containing 50g table sugar, 5g yeast extract powder, 1.88g methylparaben, and 2.5 mL of mixed propionic acid and o-phosphoric acid per liter, pH 4.2. Once loaded with 25 young flies, these vials were placed in the slots of a 32 large-slot Locomotor Activity Monitor (Trikinetics, Inc.), shown in Figure 2.4. This device has infrared beams surrounding the middle plane of each slot, allowing it to detect every time a fly walks up or down past the vial's midline. The monitor was connected to a computer, and midline-crossings were recorded every 15 minutes using the DAMSystem308X software (Trikinetics, Inc.). Flies were passed to fresh

liquid-food vials on every 3rd day. Deaths were recorded every time vials were changed, to account for differences in overall activity due to fly death. Data were later compiled with DAMFileScan111X (Trikinetics, Inc.) and used to calculate daily activity for each vial.

The second locomotor assay was run similarly to the first, except that flies were kept in plastic vials with standard agar food, rather than cotton and liquid food. Additionally, flies were only placed in the monitor for 43-45 hours at a time in the second assay, rather than 72 hours, to further reduce the possibility of food becoming sticky and interfering with fly activity. 8 replicate vials of 20-25 flies each were used for each condition, except only 5 vials were used for male [ELAV > RNAi-Prx2540 + AB], and only 4 vials for male [ELAV > RNAi-Prx2540], due to a shortage of flies. Activity measurements were conducted at age 3 and age 8 for male flies, and at age 3 and age 16 for female flies. The second age of measurement for each sex was chosen based on lifespan, since these ages correspond approximately to the onset of mortality for male and female AD flies, respectively. Consequently, AD flies at this age should already experience locomotor defects, but should not yet suffer from severe AD-induced death, thus maximizing differences in activity due to AD severity while minimizing error due to loss of flies during the experiment. For each LAM measurement, four genotypes were measured at a time: the experimental condition (ELAV > RNAi- or UAS-Prx2540 + AB), an amyloid-β control (ELAV > AB), the Prx2540 construct control (ELAV > RNAi- or UAS-Prx2540) and ELAV/+ . Vials were passed in the evening immediately before placement in the LAM, and were passed again immediately after removal from the LAM in the early afternoon 43-45 later. Vials were passed daily between measurement periods. Fly deaths were recorded at each vial passing, including before and after activity measurement, to determine the number of flies in each vial during the activity measurements. For both locomotor experiments, all fly vials and the LAM

were kept in the same 28ºC incubator used for both lifespan assays, with a 12 hour day/night cycle. Total-activity-per-fly was calculated for each vial by dividing the total number of activity counts for a vial over all 24 hours by the number of flies in that vial. In cases where one or more flies died during an activity measurement, the average number of living flies in that vial during the measurement was used for calculation of total-activity-per-fly. The average total-activity-per-fly was calculated by averaging the total-activity-per-fly of all vials of a given genotype, and standard deviation in total-activity-per-fly was also calculated from all vials of a given genotype. For vials in which some flies died during activity measurement, the standard deviation between the number of living flies at the start and at the end of the measurement was added to the standard deviation in total-activity-per-fly. Significant differences in total-activity-per-fly between genotypes were determined by Student T-test using the average and standard deviation of total-activity-per-fly, with a significance cutoff of $P = 0.05$.

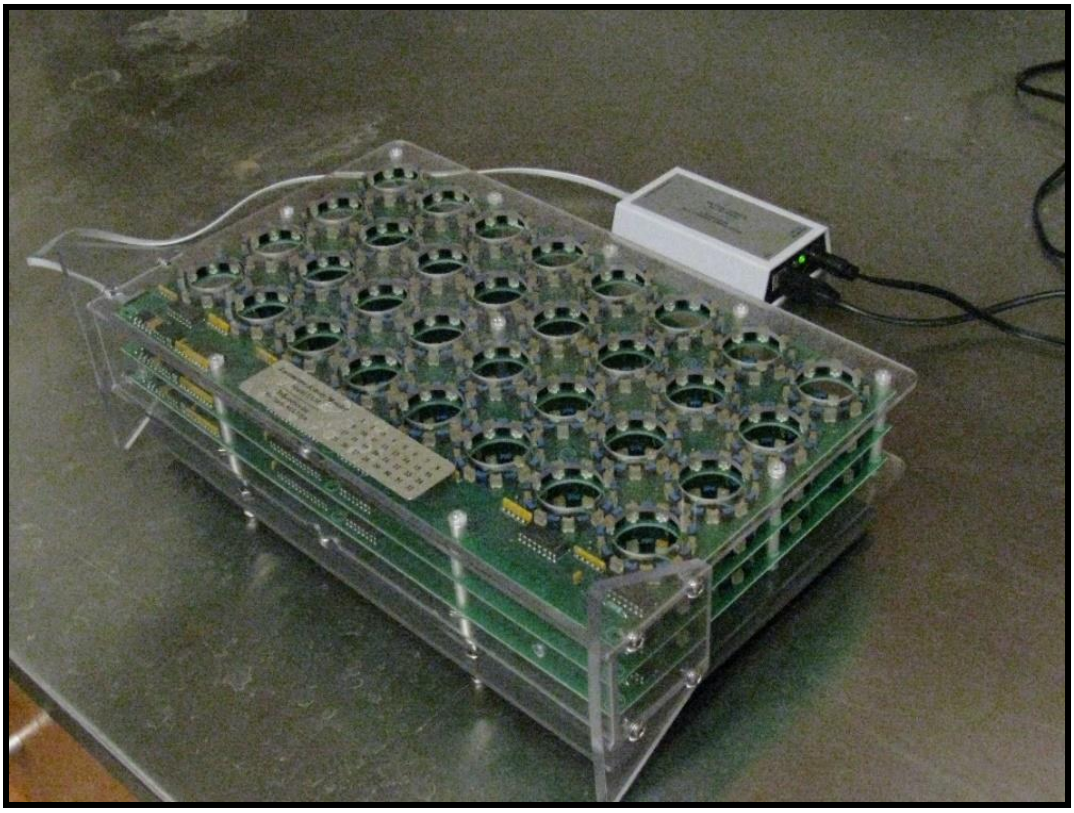

Figure 2.4 Locomotor Activity Monitor. Each of the 32 slots in this device can hold a single fly vial. The three circuit layers each support a ring of infrared sensors, although only the middle layer records the number of times flies cross its sensor beams in a given time interval.

2.9 PLA2 Inhibitor Tests

Three phospholipase A2 inhibitors were tested: MJ33 lithium salt (Sigma-Aldrich), palmityl trifluoromethyl ketone (synonym $PACOCF_3$, Calbiochem), and ASB14780 (Sigma-Aldrich). MJ33 dilutions for the first MJ33 test were prepared by reconstituting 5 mg MJ33 in 1 mL sterile water, mixing, and then aliquoting to create stock solutions at 0.5 mg/ml and 0.05 mg/ml concentrations. $PACOCF_3$ dilutions were prepared by aliquoting the stock PACOCF3 solution – 5 mg $PACOCF_3$ in 0.5 mL 95% ethanol – to create 0.1 mg/ml and 1.0 mg/ml dilutions in 95% ethanol. ASB14780 dilutions in dimethyl sulfoxide (DMSO) were prepared by

reconstituting 5 mg ASB14780 in 0.5 mL DMSO, mixing, and then aliquoting to create stock solutions at 1 mg/ml and 0.1 mg/ml concentrations. DMSO was highly toxic to *Drosophila*, so an aqueous ASB14780 stock was prepared by adding 5 mg ASB14780 to 10 mL 0.5% hydroxypropyl cellulose (HPC) in purified water, forming a suspension with small ASB14780 particles. Toxicity tests were performed by pipetting 190 μL of each inhibitor or vehicle solution onto the surface of standard agar food in plastic vials, and then gently tilting and swirling the vials until each solution covered the surface of the food completely. Vials were left upright for 24-48 hours before receiving flies, to give the solutions time to soak into the food. For the initial MJ33 test, 25 male flies (+/AB33773,Over.2540 B1, collected during preparation for the 4/6/19 lifespan assay), age 6 days, were added to each vial; the test included vials with added water, 5 mg/ml MJ33, 0.5 mg/ml MJ33, or 0.05 mg/ml MJ33, with two vial replicates per treatment. In all vials except one water vial and one 5.0 mg/ml MJ33 vial, the food surface became wet by day 4, possibly contributing to subsequent fly deaths. For the second MJ33 test, 25 male or female flies (*yw*), age 1 day, were added to each vial; the test includes vials with added water or 0.5 mg/ml MJ33, with three male vial replicates and three female vial replicates per treatment. For the PACOCF3 test, 25 male flies (*yw*), age 1 day, were added to each vial; the test includes vials with 95% ethanol (vehicle), water, 10 mg/ml $PACOCF_3$, 1.0 mg/ml $PACOCF_3$, or 0.1 mg/ml $PACOCF_3$, with two male vial replicates per treatment, except one male vial replicate for the water treatment. An ASB14780 test has been initiated with 25 male or female flies per vial, age 1 day; the test includes vials with added water, 0.5% HPC (vehicle), or 0.5 mg/ml ASB14780 in 0.5% HPC, with one male vial replicate and one female vial replicate per treatment, except two male vial replicates and two female vial replicates for the ASB14780 treatment. Vials were kept in a 25^{o}C incubator and daily deaths in each vial were recorded every evening. However, vials of

the first MJ33 test were kept at 28^{o}C for the first two days. In the second MJ33 test, flies were passed to non-treated regular food vials on day 4, then were passed to fresh treatment vials on day 5, and were also passed to fresh treatment vials on days 10 and 14.

2.10 Molecular Cloning Techniques

DH5α *E. coli* were used for all plasmid transformations. Bacteria were incubated on ice with 2-5 μL plasmid solution, then heat-shocked at 42^{o}C for 30 seconds to force plasmid uptake. Bacteria were then incubated in SOC media and plated onto ampicillin (100 mg/ml) LB agar. Transformant colonies were selected by ampicillin resistance and re-streaked on ampicillin LB agar, and each clonal colony was tested by PCR for presence of the desired plasmid. Bacterial cultures for large-scale plasmid preparations were grown in LB media. All transformation and culture experiments were performed with sterile technique.

Restriction digestions of pCFD3 and pCFD4 were performed with BbsI-HF and CutSmart Buffer (New England Biolabs), essentially following recommended BbsI-HF digestion procedures. pUASTattB was digested using FastDigest BglII, FastDigest XhoI, and 10X FastDigest Buffer (ThermoFisher) and recommended procedures. Restriction-digested plasmid fragments were isolated by gel electrophoresis: electrophoresis was performed as described before, but in gels prepared using sterilized 0.5X TAE. Desired DNA products were identified by band size, excised with sterile razors, and isolated from the agarose using QIAquick Gel Extraction kit (Qiagen). Cloning ligation steps used T4 DNA Ligase and 10X T4 DNA Ligase Buffer (New England Biolabs). The pCFD3 guide RNA was assembled from two complementary single-stranded oligonucleotides, then treated with T4 polynucleotide kinase and

10X T4 Ligase Buffer (New England Biolabs) to add phosphates to the 5’ end of each strand. Gibson assembly of pCFD4 with guide RNA insert was performed using NEBuilder HiFi DNA Assembly Master Mix (New England Biolabs), with recommended procedure. All PCR reactions used for the construction of pCFD and pUASTattB vectors were performed with Q5 High-Fidelity 2X Master Mix (New England Biolabs) to minimize mutations.

CHAPTER 3

RESULTS

3.1 Creation and Validation of *Drosophila* AD and dPrx Lines

As described in Methods, multiple AD-dPrx *Drosophila* lines were generated by crossing flies that carry an amyloid-β P-element to flies with a genetic construct for over-expression (UAS-Prx) or under-expression (RNAi-Prx) of dPrx2540 or dPrx6005. dPrx protein expression was confirmed by western blots, using the offspring of crosses between these lines and Gal4-drivers or *yw* flies. Membranes were incubated with antibodies against dPrx2540 or dPrx6005, as well as actin, to normalize for total protein per lane. Two main drivers were used: Da, shown in Figures 3.1 and 3.2, and ELAV, shown in Figures 3.3-3.5.

The first driver crosses were made to Da-Gal4 or other whole-body drivers, such as Tub, to determine which AD-dPrx over-expressor and under-expressor lines were the most effective. As shown in Figure 3.1b, crossing with Da-Gal4 mildly increased dPrx2540 expression for the AD-dPrx2540 lines, up to about 20% more than the Da/+ control. Crossing between Da-Gal4 and non-AD lines with that same dPrx2540 over-expressor construct (denoted as Da > UAS-Prx2540 in Figure 3.1b) yielded much higher expression than the AD-dPrx2540 over-expressor lines. Amyloid-β may be indirectly responsible for this difference: because the amyloid-β construct is UAS-driven, it recruits Gal4 in the nucleus for its own expression, which could limit the availability of Gal4 at the dPrx2540 construct and thus reduce UAS-Prx2540 expression.

dPrx2540 under-expression with Da-Gal4 was often more successful than over-expression, yielding up to 90% knockdown of dPrx2540 relative to the *yw* or Da/+ control. The two AD-dPrx2540 lines with the strongest dPrx2540 changes – [AB33773,Over.2540 B1] and [AB33774,RNAi-2540-8ds A1], designated "B1" and "siRNA-8 A1" in Figure 3.1, respectively – were selected for further testing.

dPrx6005 over- and under-expressors were similarly crossed to Da-Gal4 or *yw* and analyzed by western blotting for dPrx6005 expression. AD-dPrx6005 over-expressors were more potent than the AD-dPrx2540 over-expressors when crossed to Da-Gal4, yielding up to about 600% more dPrx6005 than the Da/+ control, shown in Figure 3.2. Like with the dPrx2540 over-expressors, non-AD dPrx6005 over-expressor controls crossed to Da-Gal4 produced even more dPrx6005 than the AD-dPrx6005 lines. Line [AB33773,Over.6005 A1] – "A1" in Figure 3.2 – was selected for crossing to ELAV-Gal4, as well as line [AB33774,Over.6005 B]. dPrx6005 under-expressors were also analyzed by western blot; however, dPrx6005 under-expression with Da-Gal4 was often lethal, and under-expression with weaker global drivers such as Arm-Gal4 yielded few changes in dPrx6005 levels for these lines. Nonetheless, one such line – [RNAi-6005#40;AB33774 C2] – was chosen for further testing with ELAV-Gal4, under the expectation that neuron-specific knockdown of dPrx6005 would be less damaging than the global knockdown driven by Da-Gal4.

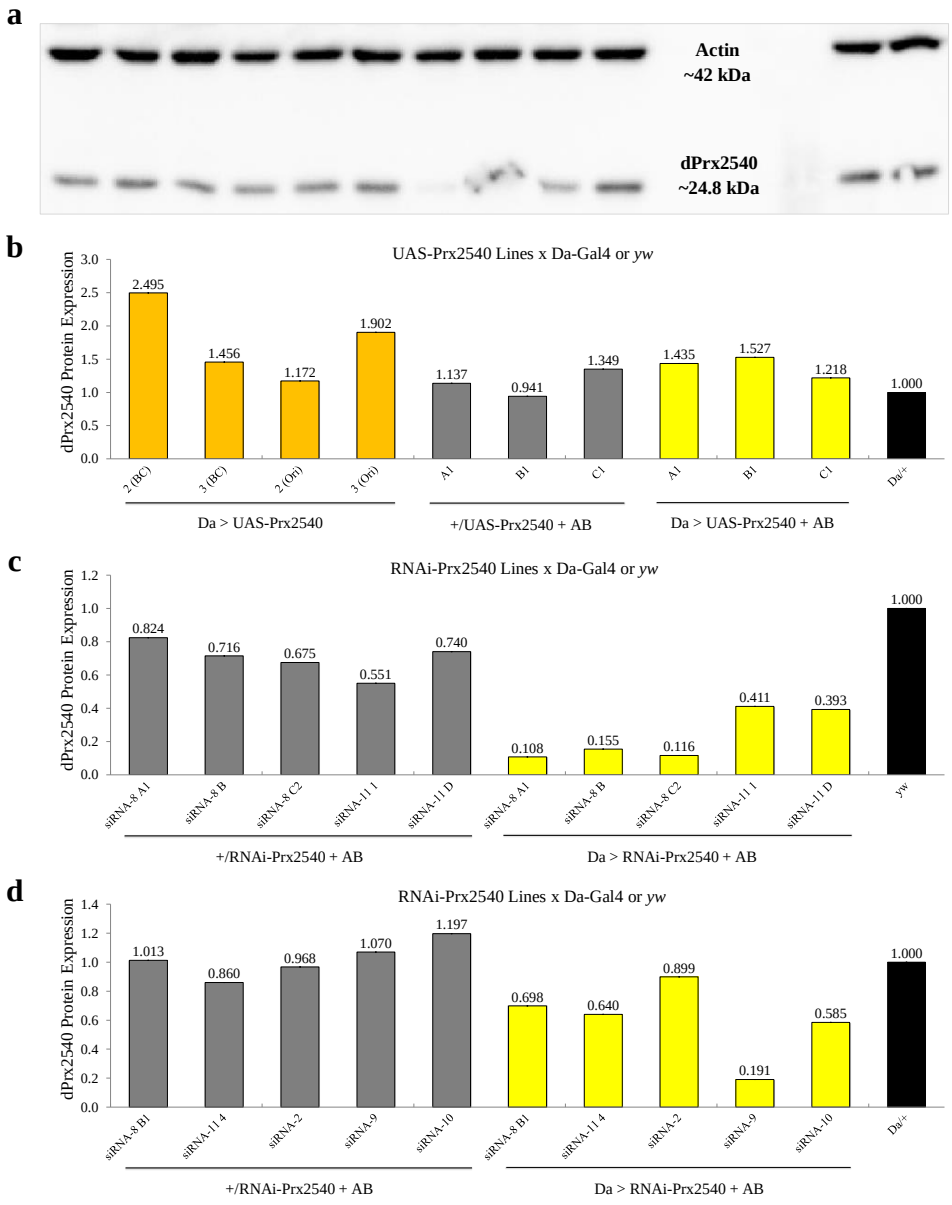

Figure 3.1 Western blot analysis of dPrx2540 over- and under-expressor lines with Da-Gal4. (**a**) Example western blot membrane, corresponding to graph (**b**). Membranes were incubated with antibodies against dPrx2540 and actin. Actin band intensities were used to normalize dPrx2540 intensity values for each lane, to account for differences in total protein input. (**b**-**d**) Quantifications of dPrx2540 expression from dPrx2540 over-expressor (**b**) and under-expressor (**c**-**d**) lines crossed to Da-Gal4 or to *yw*. Expression values are given relative to Da/+ in (**b**,**d**), and relative to *yw* in (**c**). Yellow bars indicate AD-dPrx lines crossed to Da-Gal4 (Da > X); gray indicate the same AD-dPrx lines crossed to *yw*; orange bars indicate backcrossed (BC) or non-backcrossed (ori) UAS-Prx2540 lines without amyloid-β. Letter and number abbreviations designate the specific AD-dPrx line. siRNA numbers designate which anti-dPrx2540 siRNA construct is present in each line. Protein was harvested from whole-body samples with equal numbers of males and females combined, ages 5-12 days old, except *yw* are 25-32 days old.

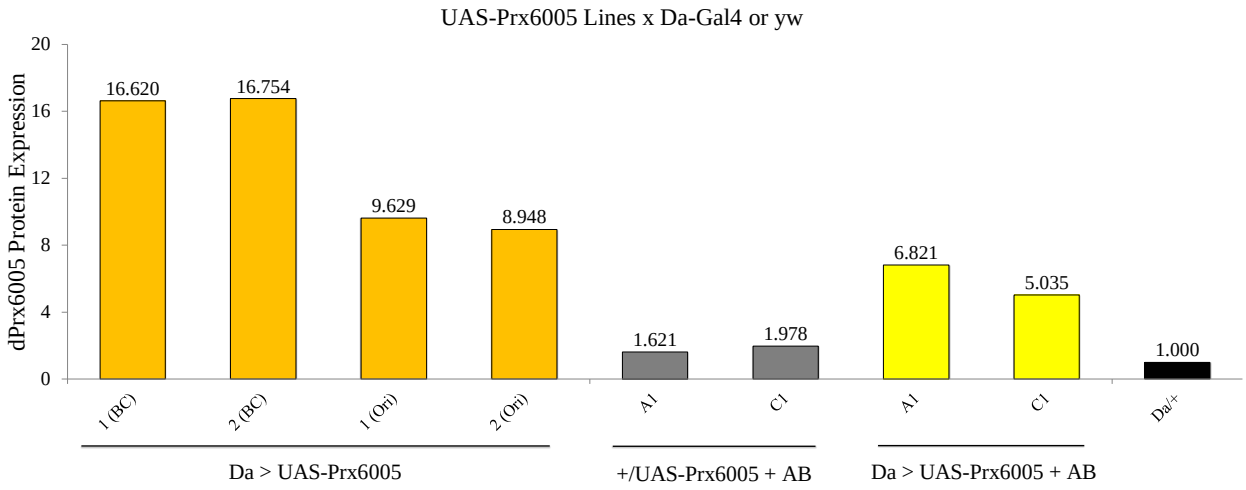

Figure 3.2 Western blot analysis of dPrx6005 over-expressor lines with Da-Gal4. Quantification of dPrx6005 expression from dPrx6005 over-expressor lines crossed to Da-Gal4 or *yw*. Expression values are given relative to Da/+ and normalized to actin, as in Figure 3.1. Protein was harvested from whole-body samples with equal numbers of males and females combined, ages 5-12 days old. dPrx6005 under-expressor lines were also crossed to Da-Gal4 for expression analysis, but all lines either failed to under-express dPrx6005 or died prematurely.

Because expression of dPrx2540 and dPrx6005 in the central nervous system was the ultimate goal for studying brain-specific Prx6 effects, dPrx2540 and dPrx6005 lines that were selected from the Da-Gal4 analyses were next crossed to driver ELAV-Gal4, which targets expression to neuronal cells. Offspring of these crosses were collected and used for western blot analysis, as well as for lifespan and locomotor studies. Protein samples were prepared from fly heads, to estimate CNS expression, by freezing the flies in liquid nitrogen and vortexing to fractionate body parts. As shown in Figure 3.3, AD-dPrx2540 over- and under-expressor lines crossed to ELAV-Gal4 produced up to about 80% more dPrx2540 and 70% less dPrx2540 than the ELAV/+ control, respectively. Because males and females were isolated separately from these crosses, expression differences between sexes were apparent in some cases. In particular,

male offspring of the cross between the control line [RNAi-2540-8ds] and ELAV-Gal4 (denoted as ELAV > RNAi-Prx2540 in Figure 3.3) do not appear to under-express dPrx2540.

The AD-dPrx6005 lines [AB33773,Over.6005 A1], [AB33774,Over.6005 B] and [RNAi-6005#40;AB33774 C2] were also crossed to ELAV-Gal4 and analyzed by western blot. As shown in Figure 3.4, the AD-dPrx6005 over-expressor lines had strong expression when crossed to ELAV-Gal4, up to about 700% more dPrx6005 than the ELAV/+ control. dPrx6005 under-expression was less extreme, up to about 70% knockdown relative to the ELAV/+ control. Also, dPrx6005 over- and under-expressor constructs appear to have 'leaky' expression – expression from the UAS-driven construct even without a Gal4 driver – as indicated by slightly elevated dPrx6005 expression levels in the +/UAS-Prx6005 Aβ lines and slightly decreased expression in the +/RNAi-Prx6005 Aβ lines lacking the ELAV-Gal4 driver.

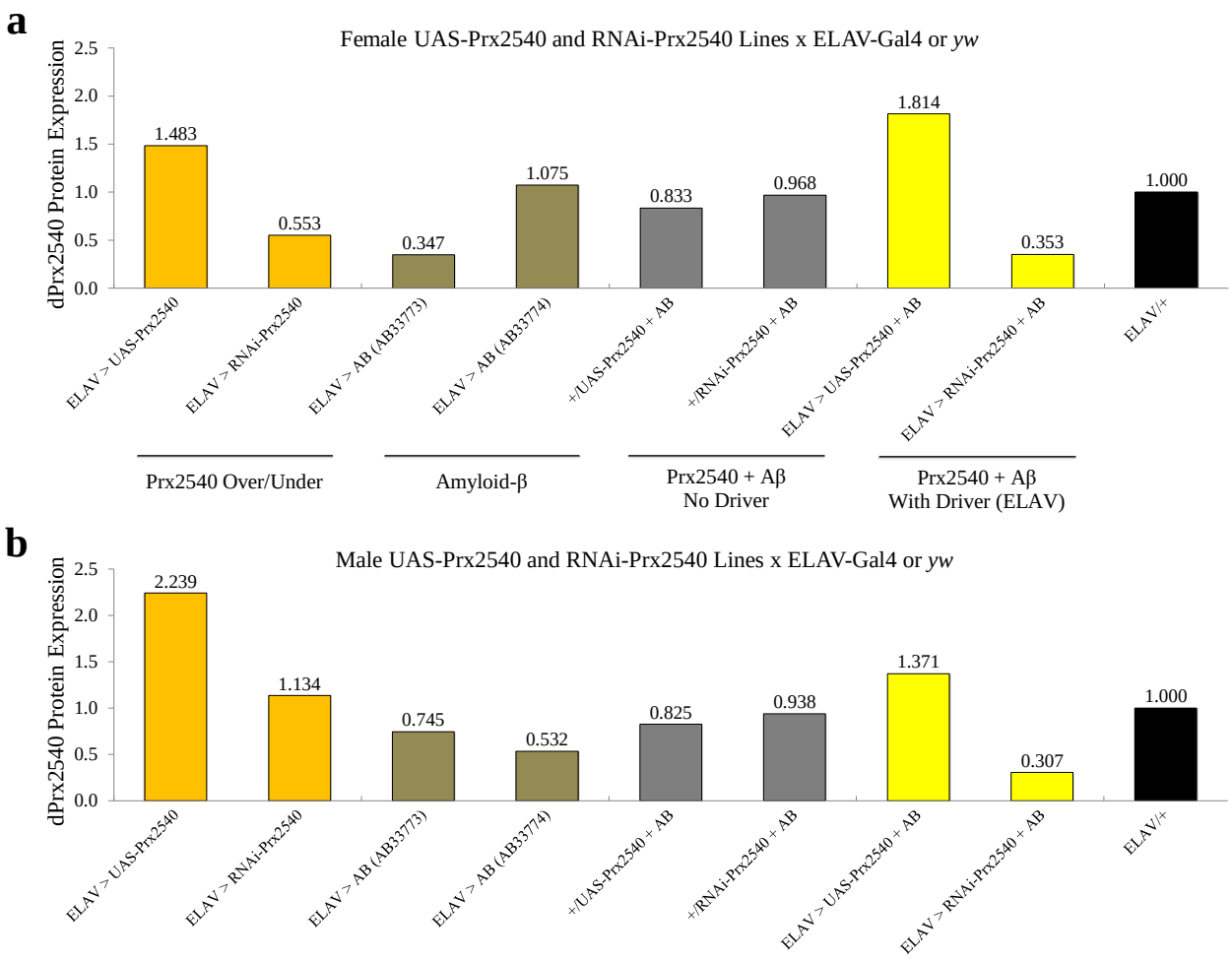

Figure 3.3 Western blot analysis of dPrx2540 over- and under-expressor lines with ELAV-Gal4. (**a**-**b**) Quantifications of dPrx2540 expression from female (**a**) or male (**b**) dPrx2540 over-expressor and under-expressor lines crossed to ELAV-Gal4 or to *yw*. Expression values are given as in Figure 3.1. Beige bars indicate amyloid-β lines without UAS- or RNAi-Prx2540, crossed to ELAV-Gal4. Aβ33773 and Aβ33774 are amyloid-β transgenes on the 2nd and 3rd chromosome, respectively. ELAV > UAS-Prx2540 + AB is [AB33773,Over.2540 B1]; ELAV > RNAi-Prx2540 + AB is [AB33774,RNAi-2540-8ds A1]. Protein was isolated from heads of females age 15-20 days old (**a**) or males age 17-22 days old (**b**).

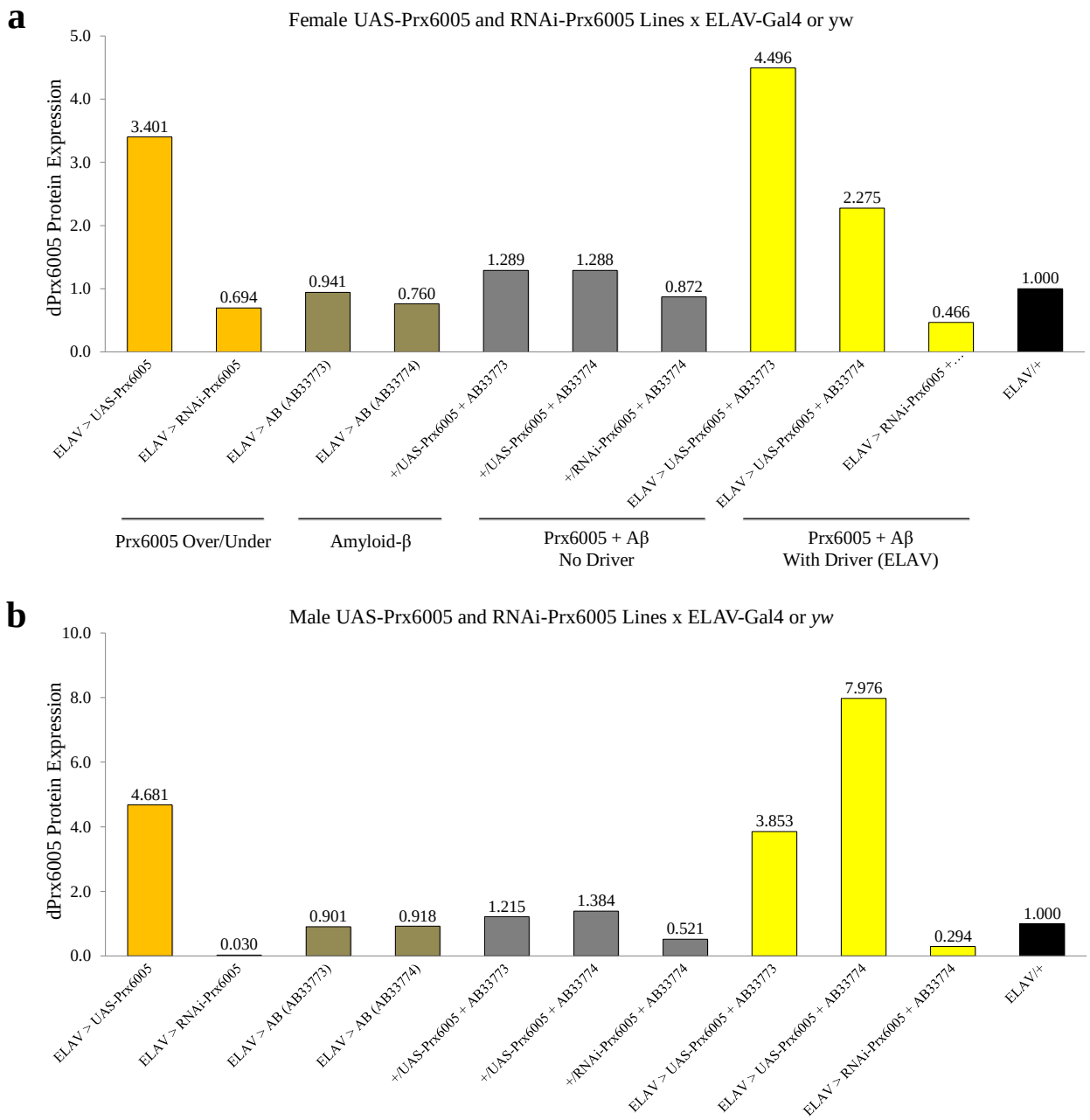

Figure 3.4 Western blot analysis of dPrx6005 over- and under-expressor lines with ELAV-Gal4. (**a**-**b**) Quantifications of dPrx6005 expression from female (**a**) or male (**b**) dPrx6005 over-expressor and under-expressor lines crossed to ELAV-Gal4 or to *yw* .Expression values are relative to dPrx6005 in ELAV and normalized to actin. Over- and under-expression in these lines when crossed to ELAV-Gal4 surpassed that of dPrx2540 expression for the dPrx2540 over- and under-expressors. Protein was isolated from heads of male or female flies, age 6-16 days old.

Because dPrx2540 over-expressor lines yielded relatively poor dPrx2540 over-expression when crossed to Da-Gal4 or ELAV-Gal4, new lines were created with homozygous expression of both ELAV-Gal4 and the dPrx2540 over-expressor construct. As shown in Figure 3.5, these homozygous driver-expressor flies produced substantially more dPrx2540 than flies with a single heterozygous ELAV-Gal4 and dPrx2540 construct, up to nearly 20 times as much dPrx2540 as the driver control. Additionally, crosses were made to create driver-expressors with an amyloid-β background, for use in future lifespan assays or other AD measurements. However, no such lines were successfully generated in the first crossing attempt, likely due to the severe toxicity of having two ELAV-Gal4 copies driving the expression of two amyloid-β constructs. A second attempt is currently underway, with a modified crossing approach that will establish the AD driver-expressors as a balanced stock – a mix of homozygotes and heterozygotes with the dPrx2540 and amyloid-β constructs. This will ensure that even if homozygotes are too sick to survive, there will still be enough heterozygotes to maintain the line and provide flies for further experiments. These lines can also be crossed to non-AD UAS-Prx2540 flies to produce offspring with one copy of ELAV-Gal4, one copy of amyloid-β, and two copies of UAS-Prx2540. Such flies would be essentially equivalent to the ELAV > UAS-Prx2540 + AB flies used in lifespan and locomotor experiments in this project, except they would presumably express even more dPrx2540.**

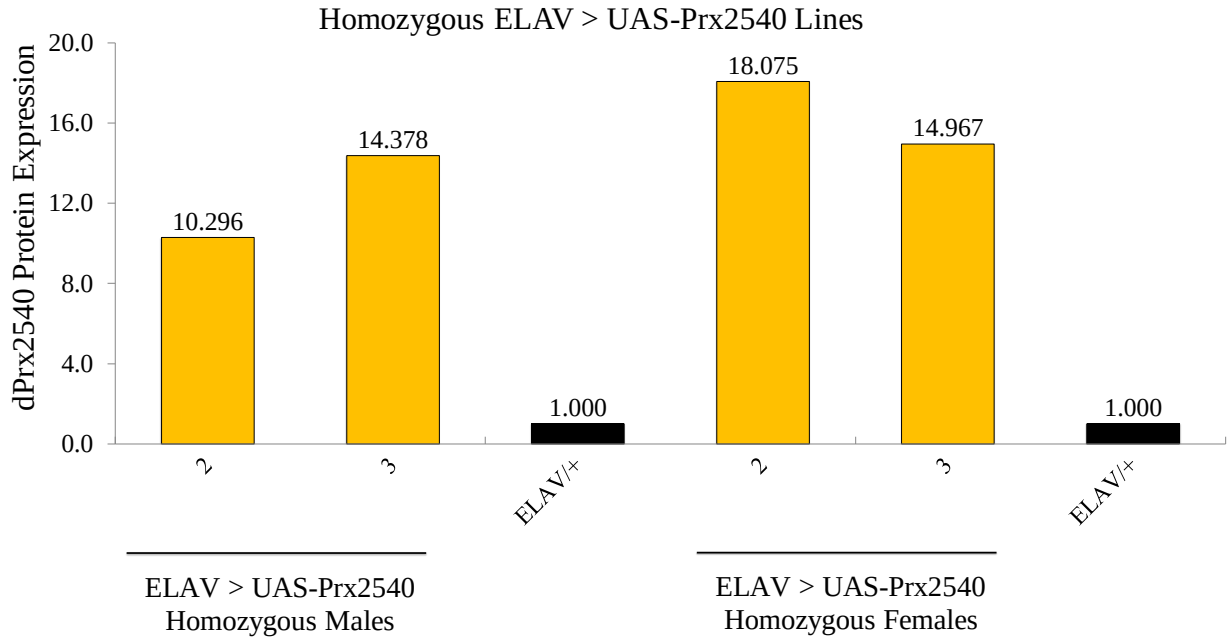

Figure 3.5 Western blot analysis of dPrx2540 homozygous driver-expressors. Quantifications of dPrx2540 protein expression are relative to ELAV/+ and normalized to actin. ELAV > UAS-Prx2540 homozygous flies possess two copies of the ELAV-Gal4 construct and two copies of the dPrx2540 over-expressor construct. Protein was isolated from heads of females or males age 20 days old.

3.2 Neuroinflammation Analysis in AD and dPrx Lines

The hypothesis predicts that changes in dPrx2540 should stimulate inflammation in the *Drosophila* brain by way of its PLA2 activity, and that this inflammatory response should drive AD progression. To measure neuroinflammation in response to dPrx2540, the heads of homozygous driver-expressor flies – with two copies of ELAV-Gal4 and two copies of the dPrx2540 over-expressor construct – were harvested, and mRNAs from the head tissue were isolated and reverse-transcribed. qPCR was then performed to measure levels of seven antimicrobial peptides (AMPs) in the brain. These proteins are innate immunity factors that activate in *Drosophila* during infection or inflammation (Shaukat, Liu and Gregory, 2015), and

they can induce neurodegeneration when over-expressed (Cao, Chtarbanova, Petersen, and Ganetzky, 2013). Consequently, the levels of expression of these proteins in dPrx2540 driver-expressor fly heads should indicate whether dPrx2540 promotes neuroinflammation.

As shown in Figure 3.6, expression of most AMPs in these flies changed little if at all relative to ELAV-Gal4 controls. Female 'Homozygous 2' flies did have significantly elevated expression of some AMPs, including *Drosomycin* and *Cecropin*, but 'Homozygous 3' actually had lower levels of several AMPs relative to ELAV. In total, these data provide insufficient evidence to conclude whether dPrx2540 exacerbates neuroinflammation. More homozygous driver-expressor lines are currently being tested for AMP levels, including lines with the other neuronal driver APPL-Gal4 in place of ELAV-Gal4. In addition to AMPs, other markers of inflammation will also be assessed, including the *Drosophila* TNFα homolog *Eiger*, and the *Turandot* family of immune- and stress-response factors. Results from this larger study should provide more conclusive evidence regarding the effects of dPrx2540 over-expression on neuroinflammation in *Drosophila*.

Figure 3.6 AMP expression in homozygous driver-expressors. Data represent mean fold-change in AMP mRNA expression relative to ELAV, ± standard deviation. Data are averaged from multiple experiments on males and females, each of which used three replicates per genotype. Attacin-AB is total expression of attacin-A and attacin-B. Homozygous 2 and Homozygous 3 are two homozygous driver-expressor lines, with two copies of ELAV-Gal4 and two copies of UAS-Prx2540. Because homozygous driver-expressor lines already have ELAV-Gal4 and UAS-dPrx2540, no crossing was performed for this experiment. mRNA was isolated from heads of females or males age 20 days old.

3.3 Lifespan Tests with AD and dPrx Lines

As discussed in section 3.1, the best AD-dPrx2540 over-expressor and underexpressor lines – [Aβ33773,over.2540 B1] and [Aβ33774,RNAi-2540-8ds A1], respectively – were selected for crossing to ELAV-Gal4, and their offspring were used for lifespan and locomotor assays to directly test the project's hypothesis. Because Prx6 and dPrx2540 have homologous PLA2 catalytic residues, it was predicted that increasing the expression of dPrx2540 in the *Drosophila* brain would increase the severity of AD-related symptoms, whereas the opposite would occur if dPrx2540 levels were decreased. In contrast, dPrx6005 should have little impact on AD, or may even yield a positive effect, due to reduced oxidative stress in the brain from its PRX activity. The simplest measurement of AD severity in *Drosophila* is lifespan. In humans, neurodegeneration from AD leads to incapacitation and systemic dysfunction, ultimately resulting in death (Alzheimer's Association, 2019). Flies with transgenic 'arctic' amyloid-β – including the Aβ33773 and Aβ33774 constructs – experience this mortality at an accelerated rate, cutting their lifespan by more than half in some cases (Crowther, Kinghorn, Miranda, Page, Curry, Duthie, Gubb, and Lomas, 2005). To determine whether dPrx2540 expression modulates AD severity, [Aβ33773,over.2540 B1] and [Aβ33774,RNAi-2540-8ds A1] flies were crossed to ELAV-Gal4 or *yw*. Additionally, the two amyloid-β lines that were used to generate these flies – lines [Aβ33773] and [Aβ33774] – were similarly crossed to ELAV-Gal4, as were the lines [over.2540] and [RNAi-2540-8ds] as controls. Offspring of these crosses were collected and passed to fresh vials daily, and deaths were counted at each passing to create a survivorship record.

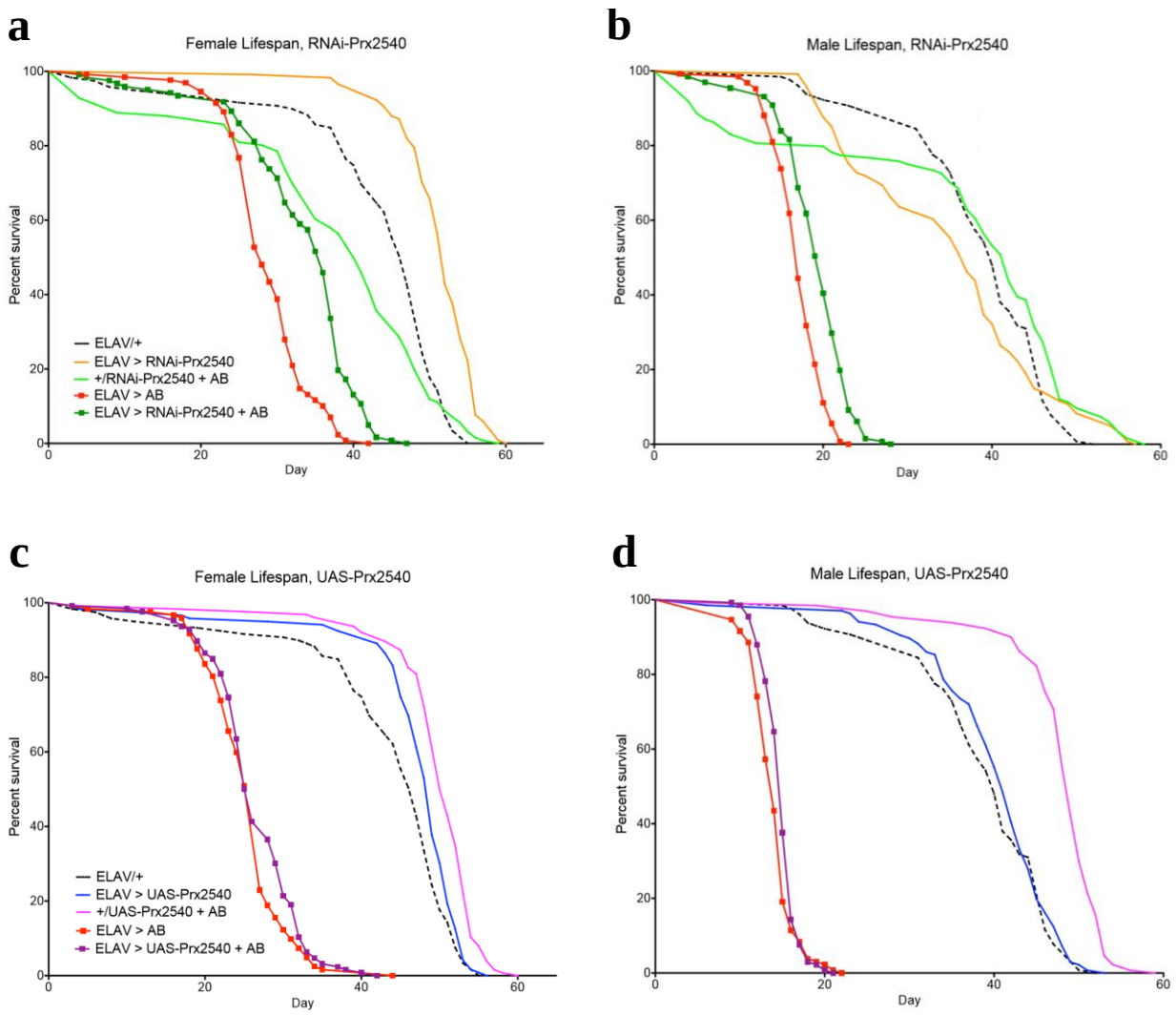

Figure 3.7 Survivorship plots for dPrx2540 and control flies from the first assay. Experimental and control lines with a dPrx2540 and/or amyloid-β construct were crossed to ELAV-Gal4 or *yw*, and 125 offspring were collected from each cross and counted daily to determine survivorship. In the RNAi-Prx2540 graphs, the amyloid-β line crossed to ELAV-Gal4 is Aβ33774; in the UAS-Prx2540 graphs, the amyloid-β line crossed to ELAV-Gal4 is Aβ33773. A reference *yw* control was also included for each sex, but not shown here. Table 3.1 quantifies median lifespan and significant differences between curves for all conditions. See Table 2.1 for more information on genotype abbreviations.

Female Lifespan		
Genotype	Median Lifespan (Days)	Significant *P* values of interest
ELAV > AB (Aβ33774)	28	
ELAV > AB (Aβ33773)	27	
ELAV > RNAi-Prx2540 + AB	36	$P < 0.0001$ (compared to ELAV > Aβ33774)
ELAV > UAS-Prx2540 + AB	25.5	n.s.
ELAV/+	47	
yw	47	
ELAV > RNAi-Prx2540	52	$P < 0.0001$ (compared to ELAV/+)
ELAV > UAS-Prx2540	49	$P = 0.005$ (compared to ELAV/+)
+/RNAi-Prx2540 + AB	40.5	$P < 0.0001$ (compared to *yw*)
+/UAS-Prx2540 + AB	50.5	$P < 0.0001$ (compared to *yw*)
Male Lifespan		
Genotype	Median Lifespan (Days)	Significant *P* values of interest
ELAV > AB (Aβ33774)	17	
ELAV > AB (Aβ33773)	14	
ELAV > RNAi-Prx2540 + AB	20	$P < 0.0001$ (compared to ELAV > Aβ33774)
ELAV > UAS-Prx2540 + AB	15	$P = 0.0091$ (compared to ELAV > Aβ33773)
ELAV/+	40	
yw	42	
ELAV > RNAi-Prx2540	37	n.s.
ELAV > UAS-Prx2540	41	n.s.
+/RNAi-Prx2540 + AB	42	n.s.
+/UAS-Prx2540 + AB	49	$P < 0.0001$ (compared to *yw*)

Table 3.1 Lifespan medians and significant differences between dPrx2540 and control flies in the first assay. Median lifespan and *P* values were calculated from the lifespan data graphed in Figure 3.7. *P* values are shown for conditions whose lifespan curves differ significantly from their relevant ELAV > AB or ELAV/+ control. *P* values were calculated using log-rank (Mantel-Cox) test.

As shown in Figure 3.7a-b and quantified in Table 3.1, male and female offspring of the [Aβ33774,RNAi-2540-8ds A1] cross to ELAV-Gal4 (abbreviated as ELAV > RNAi-dPrx2540 + AB) experienced significantly increased lifespan relative to the offspring of the cross between amyloid-β line [Aβ33774] and ELAV-Gal4 (ELAV > AB), in accordance with the hypothesis. Unexpectedly, though, flies from the [Aβ33773,over.2540 B1] cross to ELAV-Gal4 (ELAV > UAS-Prx2540 + AB) had marginally enhanced lifespan relative to their amyloid-β control, as shown in Figure 3.7c-d, although this trend was non-significant for females. As speculated in Results section 3.1, the amyloid-β transgene and the dPrx2540 constructs may compete for Gal4 availability, which could reduce amyloid-β expression in the ELAV > UAS-Prx2540 + AB flies and thereby decrease AD severity. However, the lifespan extension from dPrx2540 under-expression in AD flies is stronger than that of dPrx2540 over-expression in AD flies, which suggests that knockdown of dPrx2540 does provide a direct benefit to the survival of AD flies. Also, ELAV-driven over-expression of dPrx2540 from the UAS-Prx2540 construct is relatively limited, at only about 1.5 to 2.0 times the level in ELAV/+ for males and females, as shown previously in Figure 3.3. This indicates that the changes in lifespan due to dPrx2540 over-expression in this experiment may not reflect the changes that would be observed if dPrx2540 was over-expressed at higher levels. Once the homozygous driver-expressor lines with double ELAV-Gal4 and UAS-Prx2540 have been generated and crossed into an amyloid-β background, these flies may be used for lifespan analysis, which should provide a more rigorous test of the over-expressor effect.

Notably, ELAV > UAS-Prx2540 flies with no amyloid-β had significantly improved lifespans relative to ELAV/+ for both males and females. Like with the AD-dPrx2540 over- and under-expressors, this creates a paradox, because females of both ELAV > UAS-Prx2540 and

ELAV > RNAi-Prx2540 had improved lifespan relative to ELAV/+, which cannot be explained by competition for Gal4 since only one UAS-regulated construct was present in each of these flies. Another explanation is that other elements in the constructs may impart a survival advantage. For example, both pUAST and pWIZ – the vectors used in UAS-Prx2540 and RNAi-Prx2540, respectively – carry a w^+ marker, an *hsp*70 promoter, UAS sites, and other elements, some of which may confer greater lifespan in female flies through an unknown mechanism. Such an effect might also explain the increased lifespans of male and female +/UAS-Prx2540 + AB relative to ELAV/+. This speculation could be tested by comparing the lifespans of ELAV > UAS-Prx2540 and ELAV > RNAi-Prx2540 flies to the lifespans of ELAV > UAS and ELAV > RNAi flies that possess the UAS or RNAi vector without any dPrx2540 insertion. However, no such tests are currently underway.

A second dPrx2540 lifespan assay was performed with the same conditions as the first assay. The assay is still ongoing as of this report, so curve-comparison significance tests are not yet applicable, although median lifespans are available for groups in which 50% or more of the flies have died. Like the first assay, ELAV > RNAi-Prx2540 + AB males in the second assay had greater median lifespan than the amyloid-β control, and likewise for females to a smaller extent, as shown in Figure 3.8a-b and Table 3.2. Also like the first assay, ELAV > UAS-Prx2540 + AB flies had slightly extended median lifespan relative to amyloid-β, shown in Figure 3.8c-d, but to a lesser degree than the ELAV > RNAi-Prx2540 + AB males. Non-AD controls for both males and females have experienced less than 25% mortality up to this point, so median lifespan has yet to be reached. Together, results from the first and second lifespan assays show that both under- and over-expression of dPrx2540 in a UAS-regulated AD background reduce mortality, but to a greater extent for dPrx2540 under-expression.

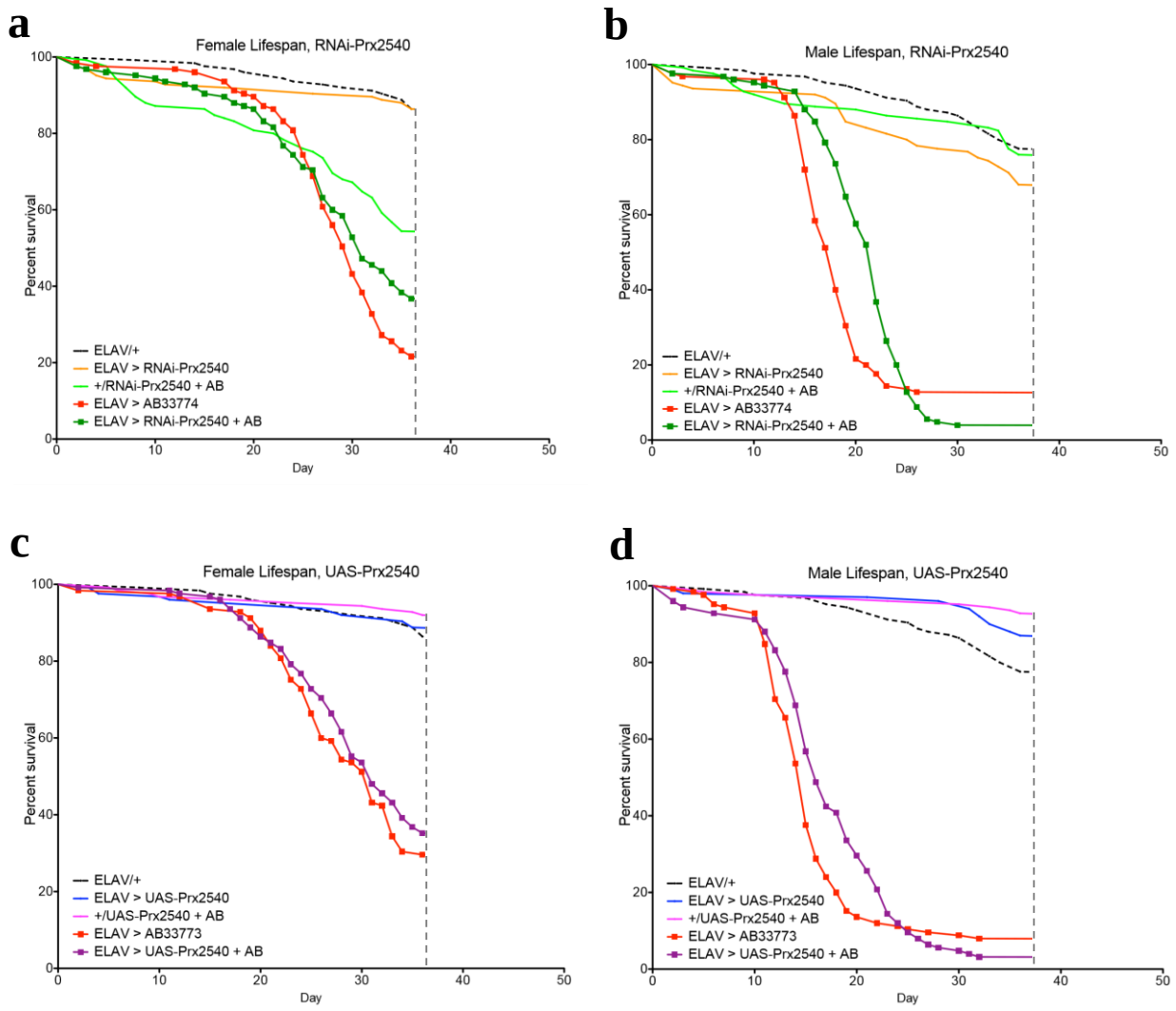

Figure 3.8 Preliminary survivorship plots for dPrx2540 and control flies from the second assay. Genotypes are identical to those of the first lifespan assay. Vertical dashed bar indicates the latest recorded death measurement. Initial number of flies is assumed to be 125 in all cases, except only 100 for male ELAV > UAS-Prx2540 due to sickness in one vial.

Female Lifespan	
Genotype	Median Lifespan (Days)
ELAV > AB (Aβ33774)	30
ELAV > AB (Aβ33773)	31
ELAV > RNAi-Prx2540 + AB	31
ELAV > UAS-Prx2540 + AB	31
ELAV/+	--
yw	--
ELAV > RNAi-Prx2540	--
ELAV > UAS-Prx2540	--
+/RNAi-Prx2540 + AB	--
+/UAS-Prx2540 + AB	--
Male Lifespan	
Genotype	Median Lifespan (Days)
ELAV > AB (Aβ33774)	18
ELAV > AB (Aβ33773)	15
ELAV > RNAi-Prx2540 + AB	22
ELAV > UAS-Prx2540 + AB	16
ELAV/+	--
yw	--
ELAV > RNAi-Prx2540	--
ELAV > UAS-Prx2540	--
+/RNAi-Prx2540 + AB	--
+/UAS-Prx2540 + AB	--

Table 3.2 Lifespan medians of dPrx2540 and control flies in the second assay. Median lifespan values were calculated from the lifespan data graphed in Figure 3.8. Median lifespan data is not available for non-AD genotypes, because fewer than 50% of these flies were dead when this data was last collected.

A similar assay was performed to determine the effects of dPrx6005 expression on the survival of AD flies. It was predicted that over-expression of dPrx6005 would not exacerbate symptoms of AD, including lifespan, because it lacks the PLA2 activity of dPrx2540 and cannot stimulate neuroinflammation through production of arachidonic acid. Conversely, dPrx6005 under-expression may increase AD severity, because the PRX activity of dPrx6005 is likely beneficial for limiting oxidative stress in the AD brain. As shown in Figure 3.9a-b and quantified in Table 3.3, however, flies from [RNAi-6005#40;AB33774 C2] crossed to ELAV-Gal4 (ELAV > RNAi-Prx6005 + AB33774) actually had better lifespan than the corresponding amyloid-β control. The two dPrx6005 over-expressor lines, [AB33773,Over.6005 A1] and [AB33774,Over.6005 B], gave mixed results when crossed to ELAV-Gal4: [AB33774,Over.6005 B] produced a small-but-significant decrease in lifespan relative to amyloid-β control for both females and males, whereas [AB33773,Over.6005 A1] had no significant effect on males (Figure 3.9d) but slightly increased lifespan in females relative to the amyloid-β control (Figure 3.9c). Also, under-expression of dPrx6005 without amyloid-β (ELAV > RNAi-Prx6005) and over-expression without amyloid-β (ELAV > UAS-Prx6005) both had a positive impact on female and male lifespan relative to the ELAV/+ control, similarly to the dPrx2540 over- and under-expressors in the first dPrx2540 lifespan assay. Overall, results from this experiment suggest that dPrx6005 has a slightly negative impact on fly lifespan in AD, contrary to the neutral or positive impact predicted by the hypothesis.

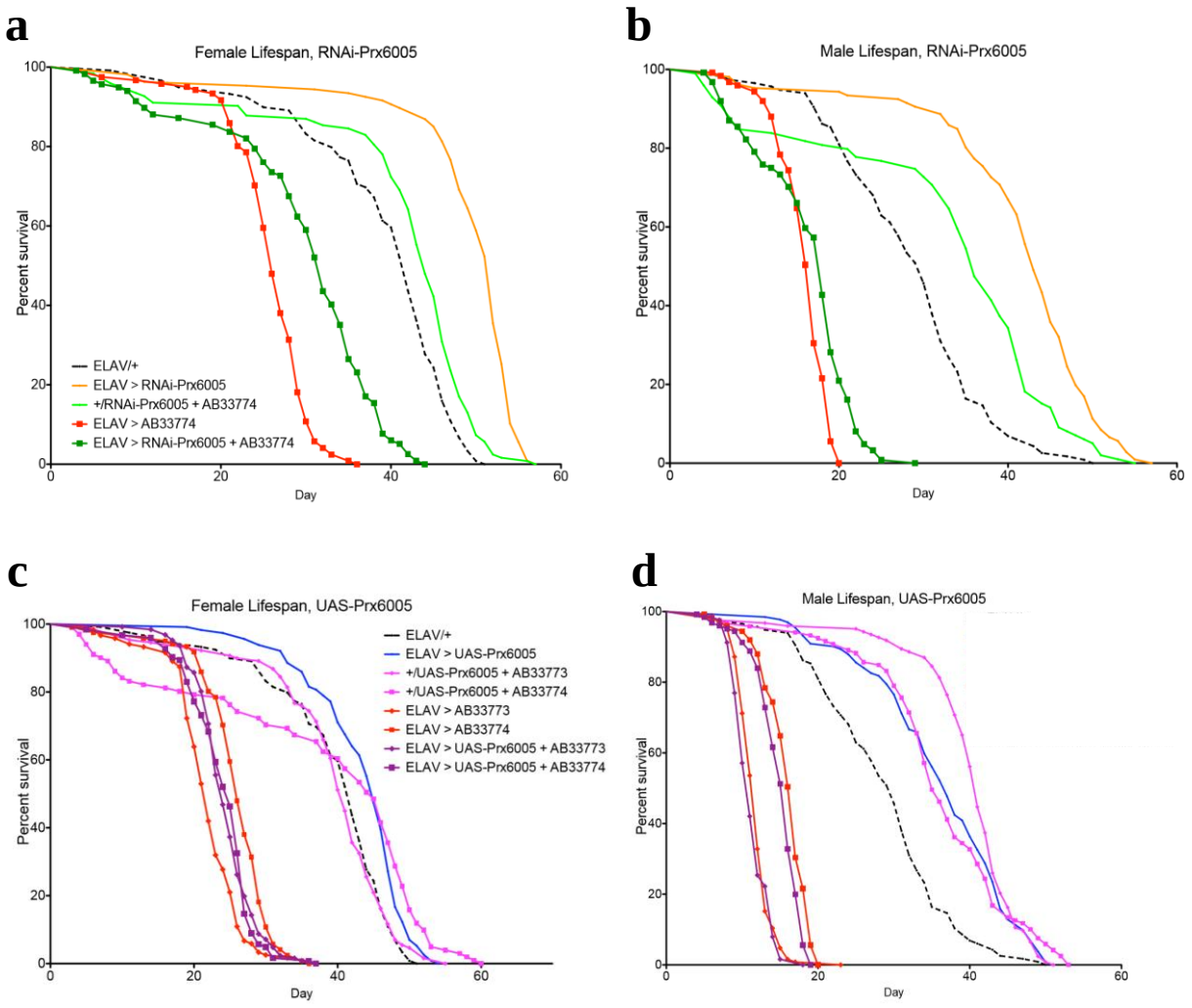

Figure 3.9 Survivorship plots for AD-dPrx6005. Numbers in parentheses indicate designations used to identify each line during the lifespan assay. The top row of graphs compares survivorship between the control lines that lack amyloid-β, while the bottom two rows compare survivorship between the [ELAV-Gal4 + Over.6005 + Aβ] or [ELAV-Gal4 + RNAi-6005 + Aβ] flies with the corresponding [ELAV-Gal4 + Aβ] control flies, and tables on the right indicate statistical calculations for the significance of differences in survivorship between these conditions.

Female Lifespan		
Genotype	Median Lifespan (Days)	Significant *P* values of interest
ELAV > AB (Aβ33774)	26	
ELAV > AB (Aβ33773)	22	
ELAV > RNAi-Prx6005 + AB33774	32	$P < 0.0001$ (compared to ELAV > AB33774)
ELAV > UAS-Prx6005 + AB33774	25	$P = 0.0004$ (compared to ELAV > AB33774)
ELAV > UAS-Prx6005 + AB33773	24	$P = 0.0001$ (compared to ELAV > AB33773)
ELAV/+	42	
yw	45	
ELAV > RNAi-Prx6005	52	$P < 0.0001$ (compared to ELAV/+)
ELAV > UAS-Prx6005	45	$P < 0.0001$ (compared to ELAV/+)
+/RNAi-Prx6005 + AB33774	44	n.s.
+/UAS-Prx6005 + AB33774	45	n.s.
+/UAS-Prx6005 + AB33773	41	$P = 0.0023$ (compared to *yw*)
Male Lifespan		
Genotype	Median Lifespan (Days)	Significant *P* values of interest
ELAV > AB (Aβ33774)	17	
ELAV > AB (Aβ33773)	12	
ELAV > RNAi-Prx6005 + AB33774	18	$P < 0.0001$ (compared to ELAV > AB33774)
ELAV > UAS-Prx6005 + AB33774	16	$P = 0.0003$ (compared to ELAV > AB33774)
ELAV > UAS-Prx6005 + AB33773	11	n.s.
ELAV/+	30	
yw	37.5	
ELAV > RNAi-Prx6005	43	$P < 0.0001$ (compared to ELAV/+)
ELAV > UAS-Prx6005	37	$P < 0.0001$ (compared to ELAV/+)
+/RNAi-Prx6005 + AB33774	36	n.s.
+/UAS-Prx6005 + AB33774	35	n.s.
+/UAS-Prx6005 + AB33773	41	n.s.

Table 3.3 Lifespan medians and significant differences for AD-dPrx6005. Median lifespan and *P* values were calculated as in Table 3.1, from the lifespan data graphed in Figure 3.9.

3.4 Locomotor Tests with AD and dPrx Lines

Loss of motor control is a hallmark of AD in humans (Alzheimer's Association, 2019) and also occurs in *Drosophila* models of the disease (Crowther, Kinghorn, Miranda, Page, Curry, Duthie, Gubb, and Lomas, 2005). As another measure of AD severity, locomotor assays were performed on the offspring of [Aβ33773,over.2540 B1] and [Aβ33774,RNAi-2540-8ds A1] flies crossed to ELAV-Gal4. These assays utilized a Locomotor Activity Monitor (TriKinetics, Inc.) that counts the number of times flies cross up and down vials in the monitor every 15 minutes. Two locomotor experiments were performed over the course of this project. In the first experiment, vials of 25 AD-dPrx or control flies were placed in the machine starting around age 10, and the flies were passed to fresh vials every third day for a period of 24 days. The vials in this experiment used 'liquid food' – a sugar-yeast medium soaked into a cotton plug at the vial's base – instead of normal agar-based solid food, because agar can melt and become hazardously sticky after two days at 28^{o}C. The liquid media had previously been used to supplement desiccated fly stocks, so it was known to be safe. As shown in Figure 3.10, however, results from this assay yielded extremely sporadic activity and few obvious changes between conditions, which provide no meaningful conclusions. Several factors likely contributed to this failure. The most critical factor was the lack of replicates: only one vial was used per condition per sex, which would have created a misleading record of fly activity if fly activeness within each condition was highly variable. Based on results from the second locomotor assay – discussed in more detail later – such variability was almost certainly present. Also, although preliminary tests indicated that healthy young flies avoid sticking to the liquid food, AD-dPrx flies in this assay often did stick to the media and die, perhaps due to AD-induced weakness. Furthermore, technical problems with the incubator disrupted fly activity seven days into the experiment.

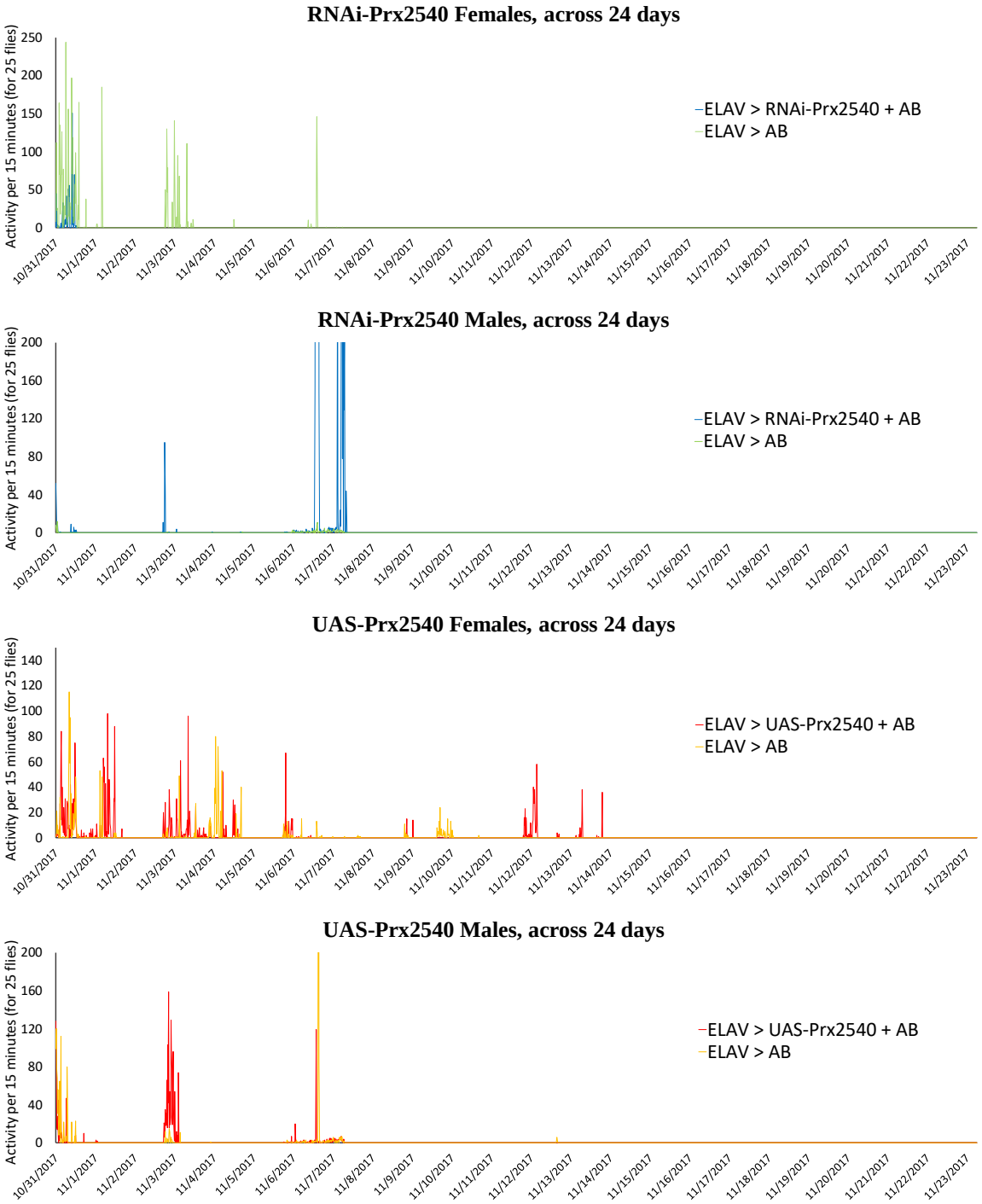

Figure 3.10 Locomotor activities of AD-dPrx and control flies from the first assay. Activity counts indicate the number of times that 25 flies in a vial crossed the vial's midline in a given 15-minute interval. Flies remained in liquid-food vials in the Locomotor Activity Monitor for 2 days at a time, and vials were passed every third day, starting on 11/2/17. Experiment was terminated on 11/24/17. Activity counts on vial-passing days are ignored. Activity counts around 11/7/17 were distorted by an incubator leak. Flies started experiment at age 8-11 days old.

To correct these errors and generate more interpretable data, a second locomotor assay was performed on the [Aβ33773,over.2540 B1] and [Aβ33774,RNAi-2540-8ds A1] flies, concurrent with the second lifespan experiment. This assay utilized normal agar-food vials rather than liquid food. However, vials were changed every 30-34 hours, which prohibited the agar from melting. Additionally, only two timepoints were measured: ages 3 days and 8 days for males, and ages 3 days and 16 days for females. The first timepoint served as a control for physical activity levels in young flies, when the effects of amyloid-β expression were presumably mild. The second timepoint was measured just prior to the onset of severe mortality in the AD flies, which begins around age 8 for males and age 16 for females, as shown previously in Figure 3.7. When not in the activity monitor, vials were passed to fresh agar food daily, and fly mortality was counted at each vial passing to account for differences in activity due to differences in the numbers of living flies per vial. Crucially, 8 vial replicates were used for each condition, except for two conditions in the ELAV > RNAi-Prx2540 males group. This provided data on the variability of fly activity between vials of the same condition, which is crucial for drawing substantive conclusions about the results.

Overall, fly activity was highly variable across all conditions of the experiment, and many ostensible differences in activity failed to reach the significance threshold. Among the 3-day-old flies, female offspring of the [Aβ33774,RNAi-2540-8ds A1] cross to ELAV-Gal4 (ELAV > RNAi-Prx2540 + AB) were significantly more active than their amyloid-β control, which in turn were more active than ELAV/+, as shown in Figure 3.11a. Male ELAV > RNAi-Prx2540 + AB flies showed a similar trend of increased activity relative to the amyloid-β control, albeit non-significantly. In contrast, young male and female offspring of the [Aβ33773,over.2540 B1] cross to ELAV-Gal4 (ELAV > UAS-Prx2540 + AB) tended to be less active than their

amyloid-β controls, though again the difference is non-significant. In older flies, a similar pattern occurred: female ELAV > RNAi-Prx2540 + AB flies had a strong trend towards being more active than the amyloid-β control, while male ELAV > RNAi-Prx2540 + AB flies had a similar but less pronounced trend, as shown in Figure 3.12a and c. Old female and male ELAV > UAS-Prx2540 + AB flies showed only minor non-significant differences from the amyloid-β controls, although males did exhibit a slight trend towards greater activity, as shown in Figure 3.12b and d. Collectively, these data suggest that dPrx2540 under-expression increases activeness in AD flies, especially young AD flies, and the opposite for dPrx2540 over-expression. However, this evidence still fails to prove whether dPrx2540 influences the severity of AD-induced locomotor activity loss, due largely to the high standard deviations in average activity that are caused by high variation in activity between the vials of each condition. Future locomotor experiments on AD-dPrx2540 or AD-dPrx6005 flies should therefore use even more replicates per group to reduce the size of standard deviations. Additionally, most of the 'old' amyloid-β controls had similar activity to ELAV/+, with the exception of the amyloid-β control for the 16-day-old ELAV > RNAi-Prx2540 + AB females. This suggests that even at 8 and 16 days old, the AD flies were not yet experiencing severe debilitation from the onset of AD. Previous experiments have shown that flies with amyloid-β begin to experience climbing deficits near their median lifespan age (Iijima, Liu, Chiang, Hearn, Konsolaki, and Zhong, 2004), suggesting that flies in this project should be measured for locomotor activity at around age 15 for males and age 27 for females.

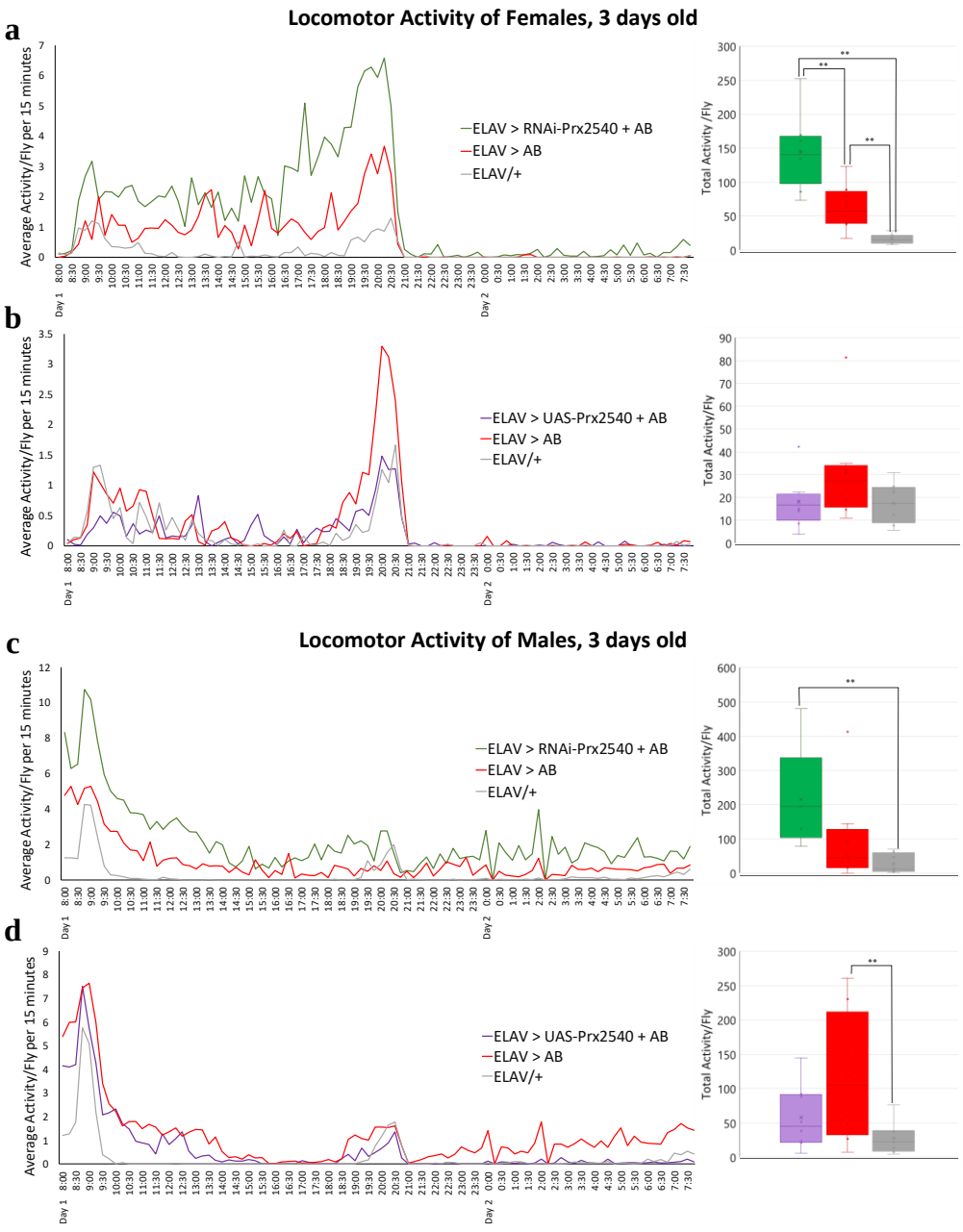

Figure 3.11 Locomotor activities of young AD-dPrx and control flies from the second assay. Activity counts were measured in a LAM as in the first locomotor activity assay. 4-8 replicate vials of regular agar-based food with 25 flies each were used per genotype. Activity was measured over a single 24 hour timeframe. Activity counts are normalized to the number of flies in each vial. At Day 1 of measurement, all flies were 3 days old. Data from females shown in (**a-b**), males shown in (**c-d**). Line graphs on the left represent the average activity per fly for each condition for every 15-minute interval of the experiment, while the box plots on the right indicate the range of average-activity-per-fly for all vials of each condition. Significance of difference in average-activity-per-fly was calculated using Student T test with significance cutoff of $P = 0.05$ for each genotype pair. All box-plot significant differences are indicated by **.

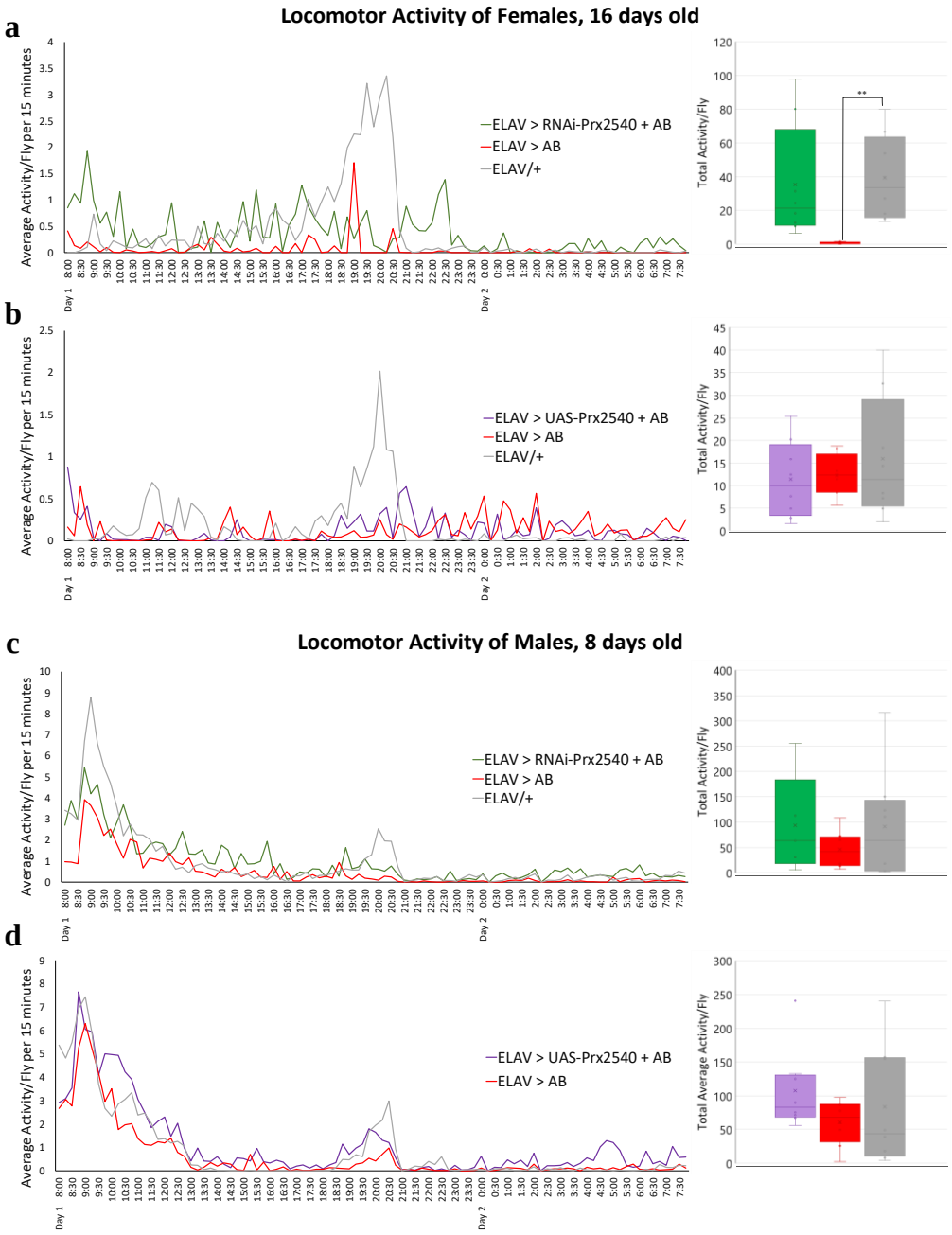

Figure 3.12 Locomotor activities of older AD-dPrx and control flies from the second assay. Activity was measured and calculated as in Figure 3.11. At Day 1 of measurement, female flies were 16 days old, and male flies were 8 days old. Data from females shown in (**a-b**), males shown in (**c-d**).

3.5 PLA2 Inhibition

According to the hypothesis, Prx6 enhances AD severity through its PLA2 activity, which generates pro-inflammatory species. If so, then inhibition of PLA2 activity in the brain may alleviate PLA2-induced neuroinflammation, which could reduce neurodegeneration and AD severity. To test this, three PLA2 inhibitors were acquired: MJ33, $PACOCF_3$, and ASB14780. MJ33 is a phospholipid analog which has been shown to inhibit the PLA2 activity of mammalian Prx6 *in vitro* (Chen, Dodia, Feinstein, Jain, and Fisher, 2000), in cell culture (Vázquez-Medina, Tao, Patel, Bannitz-Fernandez, Dodia, Sorokina, Feinstein, Chatterjee, and Fisher, 2019), and in lung tissue *in vivo* (Lee, Dodia, Chatterjee, Feinstein, and Fisher, 2014). Similarly, $PACOCF_3$ inhibits calcium-independent PLA2 enzymes *in vitro* (Conde-Frieboes, Reynolds, Lio, Hale, Wasserman, and Dennis, 1996) and works in cell culture (Yanes, Clark, Wong, Patti, Sánchez-Ruiz, Benton, Trauger, Desponts, Ding, and Siuzdak, 2010), but it also has activity against calcium-dependent PLA2 enzymes, which use a different catalytic mechanism and serve different cellular functions. ASB14780 is active against cytosolic PLA2 in enzyme assays, cell assays and mice, and it has oral bioavailability in rodents, dogs and monkeys (Tomoo, Nakatsuka, Katayama, Hayashi, Fujieda, Terakawa, and Nagahira, 2014); like $PACOCF_3$, however, ASB14780 can inhibit calcium-dependent PLA2 enzymes. Although all these compounds have been validated in cells or mammals, no studies have been published on the effects of cytosolic PLA2 inhibitors in *Drosophila*. It is therefore unknown whether these drugs are bioavailable in flies, whether they can infiltrate the brain, or whether they can enter *Drosophila* cells and modulate Prx2540 activity *in vivo*.

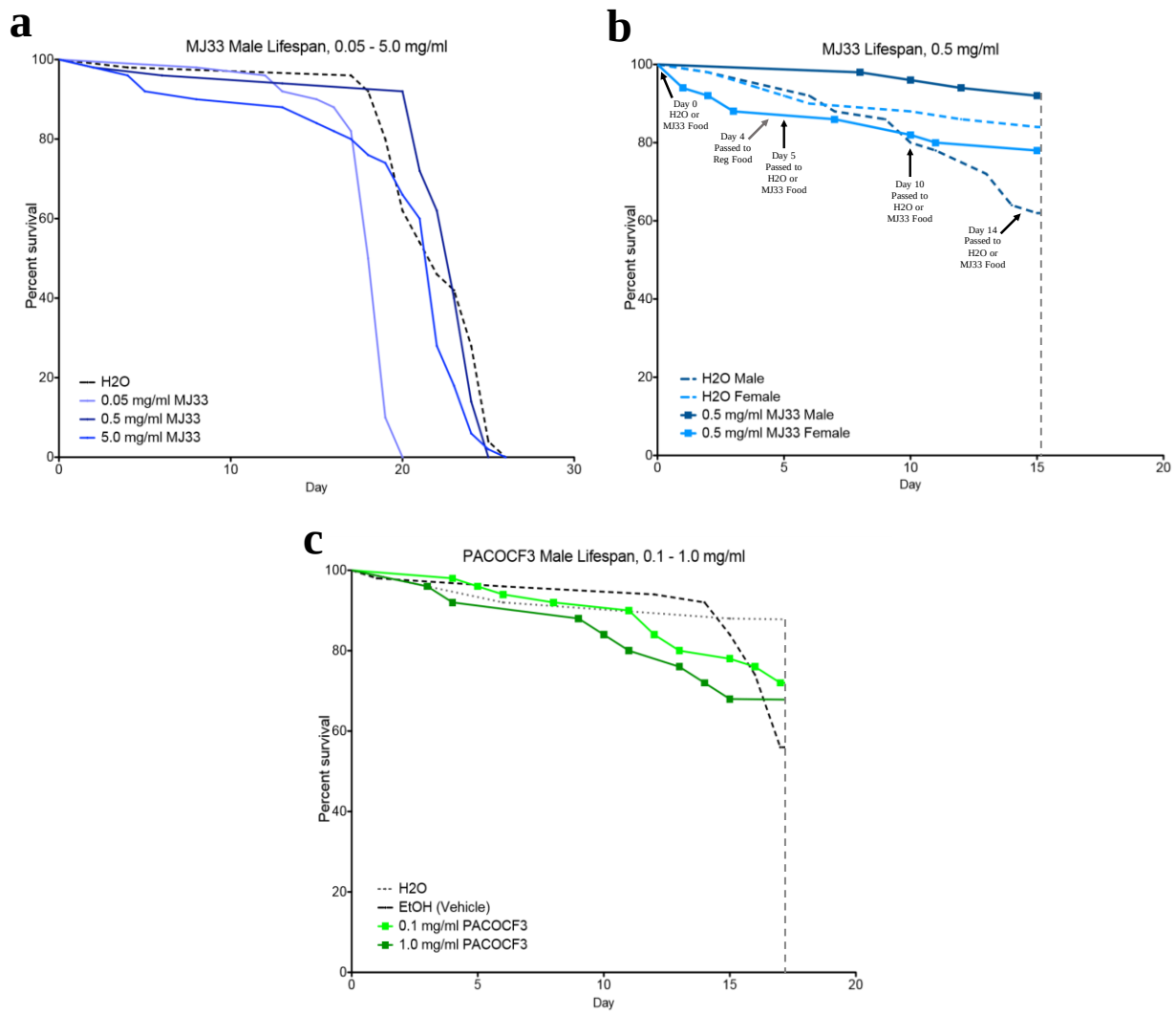

Figure 3.13 Survival of *Drosophila* on PLA2 inhibitors MJ33 and $PACOCF_3$. As in lifespan assays, flies were kept in vials at 25 flies per vial, and deaths were counted daily. Food was treated by adding190 µL of the designated inhibitor or solvent solution to the surface of regular agar food vials and incubating the vials overnight. (**a**) Survivorship of male non-AD flies (+/UAS-Prx2540 + AB) on food treated with water or varied MJ33 concentrations. Two vial replicates were used per treatment, and vials were not changed. (**b**) Survivorship of male and female non-AD flies (*yw*) on food treated with water or 0.5 mg/ml MJ33 solution. Three vial replicates were used per treatment. (**c**) Survivorship of male non-AD flies (*yw*) on food treated with water, 95% ethanol, or varied $PACOCF_3$ concentrations. Two vial replicates were used per treatment, and vials were not changed.

As a first step to determining these properties, the three inhibitors were applied to non-AD flies to evaluate toxicity and the best dose for use in future experiments. The first preliminary test measured lifespan of male non-AD flies treated with one of three MJ33 doses or vehicle (water). However, most of the vials of this test developed a sticky layer on their food surface around day 4 of the test, which may have contributed to fly deaths. Lifespan data from this test revealed no clear correlation between drug concentration and survivorship, as shown in Figure 3.13a. However, flies with 0.5 mg/ml MJ33 showed little if any mortality due to the inhibitor. A similar second test was initiated using just the 0.5 mg/ml MJ33 and water treatments, but this time with more vial replicates per treatment, with both males and females, and with fresh vials passed periodically to prevent death due to food adhesion. This MJ33 test is still underway as of this report. However, early results suggest that not only is 0.5 mg/ml MJ33 tolerable, but it may even be beneficial in a non-AD context. As shown in Figure 3.13b, males on 0.5 mg/ml MJ33 seem to outlive their water-treated counterparts. However, female flies appear to have slightly higher mortality from the drug. Once this test is complete, curve-comparison analysis should indicate whether these trends are significant, which will indicate whether 0.5 mg/ml MJ33 is safe for use in tests against AD flies. A preliminary $PACOCF_3$ test similar to the first MJ33 test was initiated and is currently underway. As with MJ33, three doses separated by factors of ten were used: 10 mg/ml, 1.0 mg/ml, and 0.1 mg/ml. 10 mg/ml $PACOCF_3$ was extremely lethal, killing all flies in both vial replicates by day 3 of the test. The 1.0 mg/ml treatment appears to be mildly toxic but not nearly as dangerous as 10 mg/ml, while the 0.1 mg/ml treatment is even less deleterious, as shown in Figure 3.13c. This suggests that lower concentrations, perhaps around 0.001-0.01 mg/ml, may prove to be the maximum non-lethal dose. The third inhibitor – ASB14780 – was initially tested in DMSO solvent, because of its poor

aqueous solubility. Because DMSO is highly toxic to flies, however, all vial replicates were killed by day 3. A new test was recently initiated using ASB14780 as a suspension in aqueous 0.5% hydroxypropyl cellulose, which has been previously used for ASB14780 oral treatments in mice (Kanai, Ishihara, Kawashita, Tomoo, Nagahira, Hayashi, and Akiba, 2016). Collectively, these data suggest that MJ33 and PACOCF3 can be used in future experiments with AD flies, at 0.5 mg/ml and less than 0.1 mg/ml, respectively. Completion of these tests, and that of ASB14780, will provide more definitive evidence concerning which concentrations are lethal and which are effectively safe in *Drosophila*.

3.6 CRISPR Deletion of Endogenous dPrx2540

The second major goal of this project was to generate flies in which the PRX or PLA2 activity of dPrx2540 is mutated, and to then combine these flies into an amyloid-β background to determine whether the PLA2 activity is specifically responsible for exacerbating AD symptoms. To complete this, two steps are required: deletion of endogenous WT dPrx2540, and addition of a UAS construct for expression of mutant or WT dPrx2540. CRISPR-mediated deletion of endogenous dPrx2540 was accomplished by expressing guide RNAs (hereafter gRNAs) and Cas9 from transgenic constructs, which were integrated into the *Drosophila* genome. This approach has been shown to improve efficiency and safety relative to methods that require injection of vectors carrying these components (Port, Muschalik, and Bullock, 2015). *Drosophila* possess three isoform duplications of dPrx2540 that are closely spaced on chromosome 2, as shown in Figure 3.14. To delete all three copies without removing other genes, two gRNAs were designed that target sequences specific to the dPrx2540-2 isoform, outside the coding region. Another gRNA was designed that targets a sequence covering the transcription start site which is

identical in all three isoform. However, this gRNA must be used last because it can also target dPrx2540-2, which would delete the whole region and all intervening genes. The plasmids pCFD3-dU6:3gRNA (hereafter pCFD3) and pCFD4-dU6:1_dU6:3tandemgRNAs (hereafter pCFD4), acquired from Addgene, were chosen to carry these gRNAs. These vectors carry a sequence downstream of the gRNA insertion site that mimics the tracrRNA structure required by Cas9, as well as promoters for ubiquitous gRNA expression, an attB sequence for recombination into the *Drosophila* genome, and a vermillion marker that can be used to screen for successful integrants. Plasmids are shown in Figure 3.15.

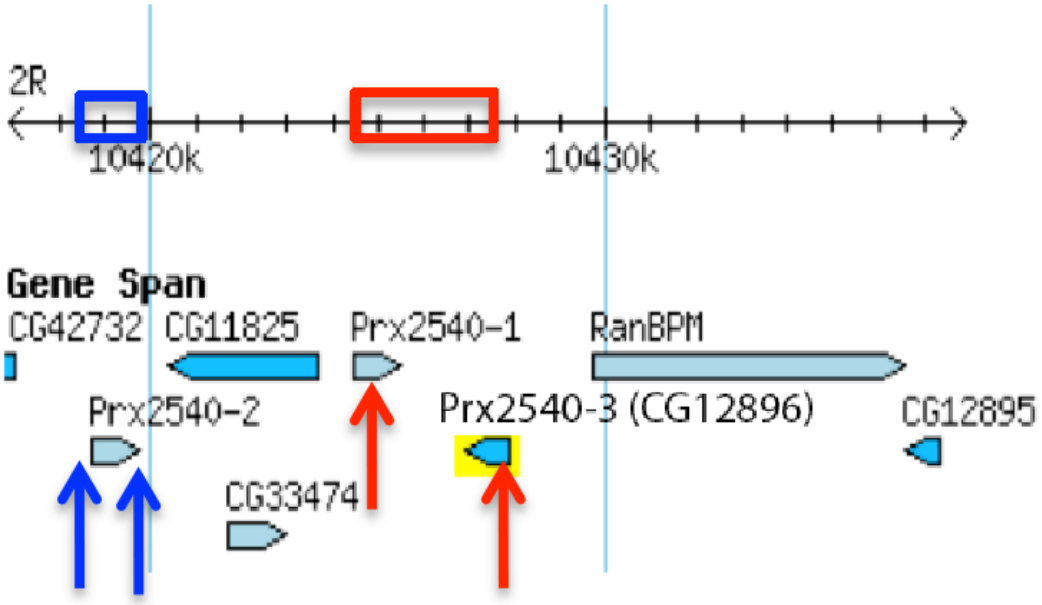

Figure 3.14 dPrx2540 isoforms and gRNA target sites. All three dPrx2540 isoforms are localized to within 10 kilobases of each other, but two genes – CG11825 and CG33474 – lie between dPrx2540-2 and dPrx2540-1/3. This means that dPrx2540-2 must be deleted separately from the others. Blue arrows indicate the sites targeted by the two guide RNAs for dPrx2540-2 deletion, while red arrows indicate the sites targeted by the guide RNA for dPrx2540-1/3 deletion. This guide RNA can also target dPrx2540-1, so dPrx2540-1 must be removed beforehand. Based on Flybase map of dPrx2540-3 (listed as CG12896), http://flybase.org/reports/FBgn0033521.

The pCFD3 gRNA for deletion of dPrx2540-1 and dPrx2540-3 has sequence **ATCAAACAGCAAGATGCGTTTGG**. This sequence was assembled as an oligonucleotide and digested with BbsI to create sticky ends. pCFD3 was likewise digested with BbsI, removing a short sequence from between the U6:3 promoter and gRNA core, and the gRNA was ligated into the gap. pCFD4 carries the two gRNAs for targeting upstream and downstream sequences specific to the dPrx2540-2 isoform, with sequences **AACGTGATCGACGTAAATAG** and **GAATGGATCACAAATGGGGAA**, respectively. A primer was created that contained the first gRNA sequence, flanked by a sequence matching the downstream end of the U6:1 promoter on one side, and a sequence matching the upstream end of the gRNA core on the other side. Another primer was similarly made for the second gRNA, this time flanked by sequences matching the U6:3 promoter and its adjacent gRNA core. PCR was performed using these primers and pCFD4 as template, which generated a 'gRNA insert' that matched the pCFD sequence from U6:1 to the second gRNA core, except with the two gRNA sequences inserted between the two promoters and gRNA cores. pCFD was then restriction-digested, and Gibson assembly was used to combine the gRNAs into the pCFD4 backbone. gRNA insertions into pCFD3 and pCFD4 were confirmed via sequencing (by Retrogen, Inc.) and injected into *Drosophila* embryos (by BestGene, Inc.) with ΦC31 for genomic integration of the plasmid. Successful integrants were identified by expression of the vermillion marker, which confers wild-type eye color when placed in a $w^{+}v^{-}$ genetic background. Homozygous lines with the pCFD4 construct were then generated, and these were crossed to flies that expresses Cas9 in the germline via the *nanos* promoter (listed as BDSC: 54591 in FlyBase). Offspring of these crosses were screened for deletion of dPrx2540-2 by PCR.

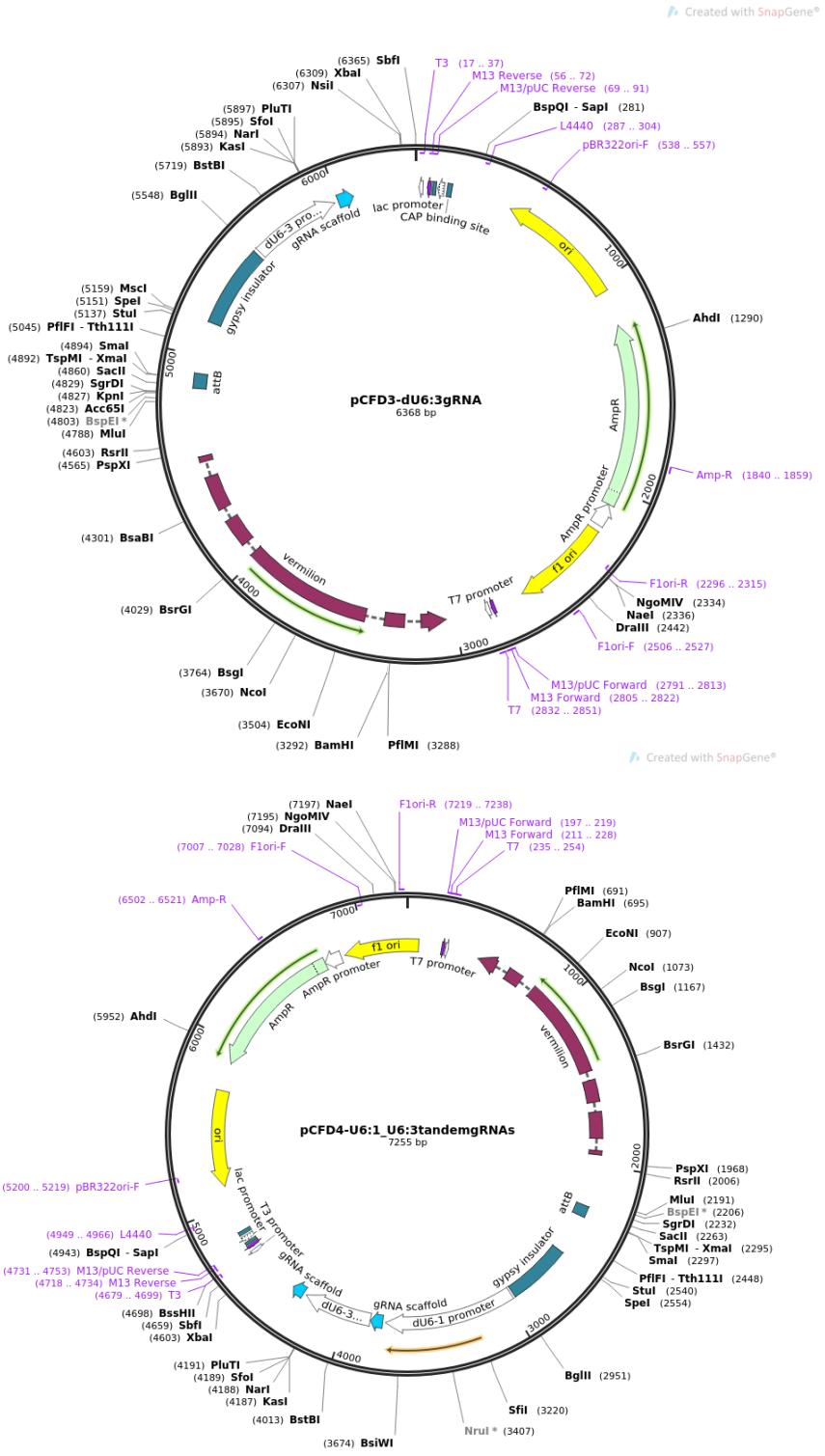

Figure 3.15 pCFD vectors for gRNA integration. gRNA sequences were inserted downstream of the U6:3 or U6:1 promoters. pCFD3 can express one gRNA, whereas pCFD4 can express two. Both vectors also carry an attB sequence for genome integration, and a vermillion marker for screens. From Addgene, https://www.addgene.org/49410/ and https://www.addgene.org/49411/.

As shown in Figure 3.16, several successful deletions were identified, and these flies were used to establish stock lines with deleted dPrx2540 (*Δ2540-2* lines). Interestingly, *Δ2540-2* flies appear phenotypically normal and express similar levels of dPrx2540 protein as control flies, as shown in Figure 3.17. This suggests that expression of dPrx2540-1 and dPrx2540-3 can compensate for loss of the other isoform. To delete dPrx2540-1 and dPrx2540-3, *Δ2540-2* flies were crossed in several steps with flies carrying pCFD3, and these flies were in turn crossed to the Nos-Cas9 line to delete dPrx2540-1 through dPrx2540-3. However, none of the initial crosses for this deletion were successful. These crosses are currently being repeated, and other methods are also being considered in case the CRISPR method is insufficient.

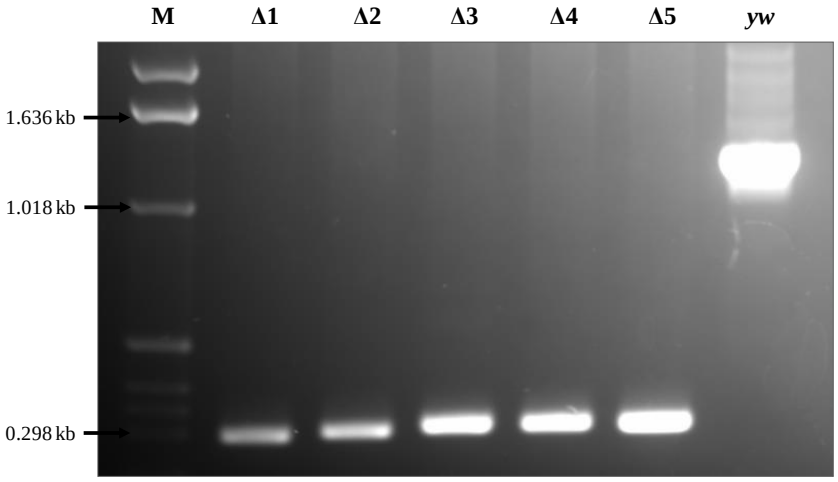

Figure 3.16 PCR gel electrophoresis for *Δ2540-2* confirmation. PCR was performed on genomic DNA of *Δ2540-2* or *yw* flies, using primers that flank dPrx2540-2. Lanes Δ1-Δ5 are DNA from five *Δ2540-2* lines, in which each line is derived from a separate Cas9-mediated dPrx2540-2 deletion event. Lane *yw* is *yw* DNA, with no dPrx2540-2 deletion. Lane M is DNA marker. The major bands of the *yw* and *Δ2540-2* samples match the sizes expected if dPrx2540 is full-length or deleted, respectively.

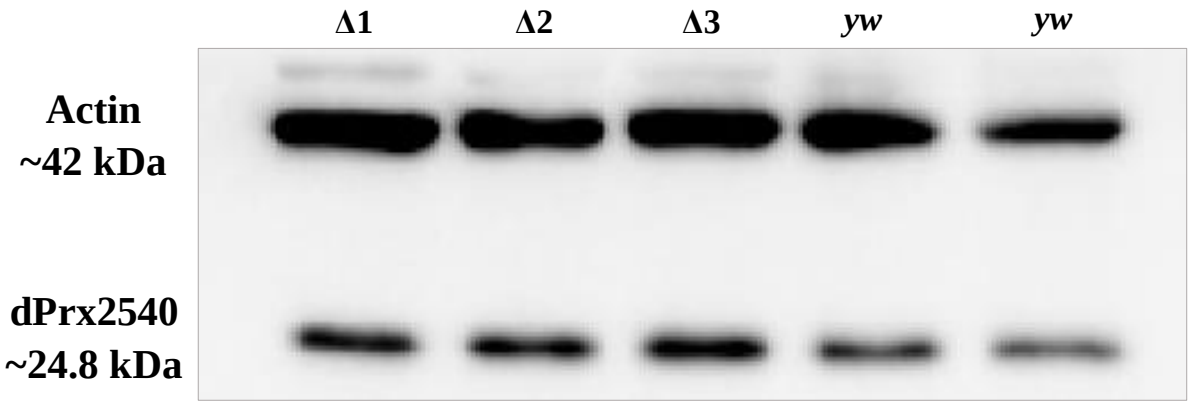

Figure 3.17 Western blot analysis of *Δ2540-2* lines. Lanes Δ1-Δ3 are protein from three *Δ2540-2* lines. Two *yw* samples were added for comparison.

3.6 Creation of PRX- and PLA2-mutant dPrx2540

Creation of the UAS-driven dPrx2540 mutants employed the same pUASTattB backbone that was used to generate dPrx2540 over-expressors prior to the start of this project. dPrx2540 mRNA was isolated and reverse-transcribed to serve as a template for mutant dPrx2540. Mutant copies of this template were then synthesized by PCR, using primers F-PRX, R-PRX, F-PLA and R-PLA. F-PRX (**TTACTCCCGTCTCCACCACTGAG**) covers the codon of the PRX catalytic Cys47 (GCA) but with a single mismatch, at the underlined C. F-PLA (**CATCAGTCCGGCCCATAAGGTGC**) covers the codon of the Asp140 at the PLA2 active site (GAC) with a single mismatch at the underlined C. R-PRX and R-PLA are the exact reverse-complement sequence of F-PRX and F-PLA, respectively, including the mismatches. To generate PRX-mutant dPrx2540, PCR was performed on dPrx2540 cDNA with the F-PRX primer, and with a reverse primer that covers the downstream end of dPrx2540, plus an overhanging sequence that includes an XhoI restriction site. Another reaction was performed with R-PRX and a forward primer covering the upstream dPrx2540 end, which introduces a

BglII restriction site. These reactions generated PCR products that cover both halves of dPrx2540, overlap over the PRX site, and introduce restriction sites at the gene's ends. Combining these PCR products and polymerase together allowed the products to bind each other and serve as primers for generation of full-length PRX-mutant dPrx2540. Because of the introduced restriction sites, BglII and XhoI were then used to digest the mutant gene and pUASTattB, and the mutant gene was ligated into the plasmid backbone to create a pUASTattB vector with PRX-mutant dPrx2540. A similar process was used to generate pUASTattB with PLA-mutant dPrx2540, using the F-PLA and R-PLA primers. Mutant pUASTattB-2540 vectors were transformed into bacteria, isolated, and injected into *Drosophila* embryos (by BestGene Inc.) and screened for successful integration. Multiple integrant lines have been received and are currently being de-contaminated. Afterwards, these flies will be tested for mutant pUASTattB-2540 using PCR with primers flanking the purported integration site.

CHAPTER 4

DISCUSSION

4.1 Analysis of Prx6 Homologs in *Drosophila* AD

In this project, *Drosophila* models of Alzheimer's disease were used to test the hypothesis that Prx6 exacerbates AD using its PLA2 activity. This required generation of several AD-dPrx fly lines that concurrently express amyloid-β and over- or under-express one of two *Drosophila* Prx6 homologs, dPrx2540 and dPrx6005, which was confirmed by western blotting. Because dPrx2540 is closely homologous to human Prx6, including at its conserved PRX and PLA2 active sites, it was predicted that dPrx2540 over-expression would exacerbate AD-related symptoms in AD flies via its PLA2 activity, and that the opposite would occur if dPrx2540 were knocked down. By this same logic, dPrx6005 should not produce such negative effects due to its lack of crucial PLA2 residues, and may even ameliorate AD severity by reducing oxidative stress with its PRX activity. To test these predictions, AD-dPrx flies and relevant controls were crossed to Gal4 drivers, and the offspring were tested for differences in lifespan and locomotor activity, which are severely attenuated in human and *Drosophila* models of AD. Results of these experiments are summarized in Table 4.1.

AD Phenotype Summary		
Genotype	Lifespan Assay	Locomotor Assay
AD with dPrx2540 over-expression	Small ↑ (n.s. for ♀)	↓ in young (n.s.)
AD with dPrx2540 under-expression	Moderate ↑	↑ in young (n.s. for ♂), ↑ in old (n.s.)
AD with dPrx6005 over-expression	Possibly ↓, mixed results	--
AD with dPrx6005 under-expression	Moderate (♀) or Small (♂) ↑	--

Table 4.1 Summary of AD phenotypic assay results. Arrows indicate an increase or decrease in lifespan or locomotor activity relative to the relevant amyloid-β control. n.s. indicates trends toward increased or decreased lifespan/activity that failed to reach statistical significance. Sexes are noted individually in cases where results differed between males and females.

The lifespan and locomotor data suggest that dPrx2540 under-expression has a beneficial effect on survival and activity in the context of AD. However, dPrx2540 over-expression also provided a slight lifespan extension to AD flies, although activity actually decreased in young flies and changed little in older flies. As discussed previously, the lifespan improvements seen in both the dPrx2540 under- and over-expression AD lines crossed to ELAV-Gal4 may be caused by decreased expression of UAS-driven amyloid-β in these flies, due to the UAS-driven dPrx2540 constructs competing with amyloid-β for Gal4 binding. Locomotor activity could be similarly affected. Lifespan or locomotor assays with flies carrying UAS-driven amyloid-β and an innocuous UAS transgene would establish whether the presence of a second UAS construct intrinsically reduces expression at the amyloid-β element. If Gal4 competition does decrease amyloid-β levels, then non-UAS amyloid-β constructs should be combined with the dPrx2540 construct lines to test the project's hypothesis. Overall, the dPrx2540 under-expressors appear to confer a greater survival and activity advantage in AD flies than that conferred by dPrx2540

over-expression. These data therefore provide some support for the hypothesis, although the Gal4 competition question must be answered before any permanent conclusions can be drawn.

The dPrx6005 lifespan data suggest that dPrx6005 may be detrimental in AD, despite the presumed absence of PLA2 activity in this enzyme. dPrx6005 under-expression was beneficial to AD fly survival, whereas over-expression decreased lifespan in males and in one female over-expression group. dPrx6005 under-expression without AD also greatly improved lifespan relative to the ELAV/+ control, although over-expression also gave a significant increase. These results suggest that dPrx6005 may actually be harmful in the context of AD, contrary to the hypothesis. It may be useful to repeat this assay in the future, especially due to the positive lifespan effects observed in both under- and over-expression of dPrx6005 without amyloid-β.

4.2 Other dPrx2540 Tests

Because the hypothesis predicts that Prx2540 drives AD severity through enhanced neuroinflammation, RT-qPCR was performed to quantify inflammatory markers in the heads of homozygous 'driver-expressor' flies possessing two ELAV-Gal4 drivers and two constructs for dPrx2540 over-expression. With a few exceptions, most AMPs that were examined showed no positive correlation between dPrx2540 expression and inflammation in the two homozygous driver-expressor lines tested. Contrary to the hypothesis, this suggests that dPrx2540 does not upregulate inflammation in the *Drosophila* brain. Current work is focused on testing more driver-expressor lines, including lines with the neuronal driver APPL-Gal4 in place of ELAV-Gal4, and also on quantifying expression of non-AMP inflammatory markers such as Eiger. Another approach currently in development is the use of glia-specific Gal4 drivers such as Repo-

Gal4. Because glial cells mediate neuroinflammation and are the main cells that over-express Prx6 in human AD (Power, Asad, Chataway, Chegini, Manavis, Temlett, Jensen, Blumbergs, and Gai, 2008), using a glial driver with the UAS-Prx2540 construct may have a greater impact on driving inflammation in the *Drosophila* brain.

As an alternative approach to mitigating dPrx2540 PLA2 activity, three cytosolic PLA2 inhibitors with known efficacy against cell and mammalian targets were acquired and tested against *Drosophila* to determine toxicity. One inhibitor, MJ33, appeared to provide some benefit to lifespan even without AD in males at moderate concentrations, but with low toxicity in females. $PACOCF_3$ was toxic at all measured concentrations, but its low toxicity at its lowest dose suggests that it may be safe at a ten-fold lower concentration. A third inhibitor, ASB14780, is currently being tested in aqueous suspension, and results should indicate whether this compound can also be used safely in *Drosophila*. Establishing safe concentrations for these drugs lays the groundwork for future studies in which these inhibitors may be tested against AD flies with or without dPrx2540 over-expression. According to the hypothesis, treatment with effective PLA2 inhibitors should alleviate AD symptoms in flies with dPrx2540, by interfering with arachidonic acid production by dPrx2540 and attenuating the generation of pro-inflammatory species. However, there are several potential drawbacks to this approach. Cytosolic PLA2 inhibitors – including those used in this project – often have activity against multiple classes of PLA2 enzymes, which can mediate non-inflammatory functions such as glutamate-receptor and platelet activity (Ong, Farooqui, Kokotos, and Farooqui, 2015). Even among the calcium-independent (iPLA2) PLA2 proteins, of which Prx6 is a member, there are several enzyme isoforms that serve distinct roles in the brain. This means that any effects of the PLA2 inhibitors in flies may not be attributable to their action against Prx6-mediated

inflammation. Additionally, the pharmacokinetics of these drugs in *Drosophila* are unknown, so many more tests are needed to confirm whether they can enter the brain and reach dPrx2540 inside cells. Because *Drosophila* possess a blood-brain barrier that can block drugs in the hemolymph from crossing into the central nervous system (Zhang, Zhifeng, Arnold, Artiushin, and Sehgal, 2018), this unfortunately makes it more likely that PLA2 inhibitors will be unable to reach neurons from circulation. Prx6 has also been shown to play major roles in non-neuronal tissues (Fisher, 2011), so PLA2 inhibitors likely affect these tissues as well. Overall, this makes PLA2 inhibition a potentially beneficial strategy for targeting AD-related neuroinflammation, but it is challenging to target Prx6 specifically and determine whether any effects are due to Prx6 inhibition in the brain.

4.3 Creation of dPrx2540 Knockouts and Mutant Alleles

One endogenous copy of dPrx2540 – dPrx2540-2 – was successfully deleted from the *Drosophila* genome, using a custom guide-RNA vector and Cas9 expressed in the germline. However, initial attempts to delete dPrx2540-1 and dPrx2540-3 using a second guide RNA have thus far been unsuccessful. Several possibilities may explain this failure. As shown in Figure 3.8, the genomic region comprising dPrx2540-1 and dPrx2540-3 is substantially larger than dPrx2540-2, which lowers the chances that non-homologous end-joining will successfully repair the deletion after cleavage by Cas9. More crossings between Cas9 flies and flies carrying the gRNA vector are currently being prepared, to improve the chances that a successful deletion will occur. Another possibility is that dPrx2540-1-3 region forms a secondary structure. As shown in Figure 3.8, dPrx2540-1 and dPrx2540-3 are head-to-tail duplications, with virtually identical sequences extending several kilobases in either direction. This may cause nucleotides in one

strand of dPrx2540-1 to base pair with the complementary opposite strand in dPrx2540-3, forming a hairpin loop. DNA looping could interfere with polymerase activity during the PCR experiments used to confirm dPrx2540-1/dPrx2540-3 deletion, giving a false negative result, or it could interfere with the binding of Cas9 to its guide-RNA target sequences, preventing the deletion from occurring altogether. The former possibility is currently being addressed using new primers spaced farther outside the repetitive dPrx2540-1-3 region, and a polymerase fused to a helicase domain that can unwind DNA secondary structures. The latter possibility is more challenging, but it might be resolvable using guide RNAs targeting sequences outside the repetitive region, or by using a combination of other gRNAs targeting different sites. Recognition and cleavage by Cas9 can also be disrupted by a closed chromatin state (Jensen, Fløe, Petersen, Huang, Xu, Bolund, Luo, and Lin, 2017). As indicated by previous RNA-seq data (see modENCODE Anatomy RNA-Seq data in http://flybase.org/reports/FBgn0033520 for dPrx2540-1 and http://flybase.org/reports/FBgn0033521 for dPrx2540-3), dPrx2540-1 and dPrx2540-3 are expressed at low to moderate levels in the adult germline, which suggests that these genes may be organized into heterochromatic regions that are inaccessible to Cas9. However, dPrx2540 protein expression in Δ2540-2 flies is close to normal levels, as shown in Figure 4.1. This suggests that isoforms dPrx2540-1 and dPrx2540-3 contribute substantially to normal dPrx2540 expression, which would likely require a relatively open chromatin state for transcription. Like with DNA secondary structures, the problem of local heterochromatin can be addressed using gRNAs that target sites further outside the dPrx2540-1-3 region, which may be less tightly condensed.

The PRX and PLA2 mutant alleles of dPrx2540 have been generated in vectors and have been injected into *Drosophila* embryos. Successful integrants will be continuously maintained

until a complete dPrx2540 knockout has been generated, at which point the integrated dPrx2540 will be crossed into the dPrx2540-null background. These flies will then be crossed into an amyloid-β background and tested for differences in AD-related symptoms, including lifespan and locomotor activity, to determine the effects of Prx6 PLA2 ablation on AD.

4.4 Conclusions

This goal of this project was to determine whether Prx6 homologs mediate AD symptoms in *Drosophila* by way of PLA2 activity. Lifespan and locomotor tests of flies with both amyloid-β and over- or under-expression of dPrx2540 – the Prx6 homolog with PLA2 activity – suggest that dPrx2540 may indeed negatively contribute to the disease. However, analysis of immune factors in *Drosophila* brains revealed few major changes in neuroinflammation caused by dPrx2540 over-expression, contrary to the hypothesis, and lifespan assays using flies that over- or under-express the non-PLA2 Prx6 homolog suggest that this enzyme may also be detrimental in AD. As another approach toward testing the hypothesis, CRISPR-Cas9 methodology has been used to target endogenous dPrx2540 isoforms for deletion, and dPrx2540 mutant alleles with ablated PRX or PLA2 activity have been generated and integrated into the *Drosophila* genome. Once completed, flies carrying these mutant alleles and lacking endogenous dPrx2540 can be crossed into an amyloid-β background. These lines can then be used for lifespan, locomotor, or other assays of AD phenotypes, to further assess the role of Prx6 PLA2 activity in AD.

REFERENCES

Alzheimer's Association (2019). 2019 Alzheimer's disease facts and figures. *Alzheimer's & Dementia*, 15(3): 321.

Bischof, J., Maeda, R., Hediger, M., Karch, F., Basler, K. (2007). An optimized transgenesis system for *Drosophila* using germ-line-specific φC31 integrases. *PNAS*, 104(9): 3312-3317.

Cao, Y., Chtarbanova, S., Petersen, A., Ganetzky, B. (2013). Dnr1 mutations cause neurodegeneration in *Drosophila* by activating the innate immune response in the brain. *PNAS*, 110(19): E1752-E1760.

Chen, J.W., Dodia, C., Feinstein, S.I., Jain, M.K., Fisher, A.B. (2000). 1-Cys Peroxiredoxin, a Bifunctional Enzyme with Glutathione Peroxidase and Phospholipase A_2 Activities. *The Journal of Biological Chemistry*, 275(37): 28421-28427.

Chen, Z., Zhong, C. (2014). Oxidative stress in Alzheimer's disease. *Neuroscience Bulletin*, 30(20): 271-281.

Chowdhury, I., Mo, Y., Gao, L., Kazi, A., Fisher, A.B., Feinstein, S.I. (2009). Oxidant stress stimulates expression of the human peroxiredoxin 6 gene by a transcriptional mechanism involving an antioxidant response element. *Free Radical Biology and Medicine*, 46(2): 146-153.

Conde-Frieboes, K., Reynolds, L.J., Lio, Y.-C., Hale, M.R., Wasserman, H.H., Dennis, E.A. (1996). Activated Ketones as Inhibitors of Intracellular Ca^{2+}-Dependent and Ca^{2+}-Independent Phospholipase A_2. *Journal of the American Chemical Society*, 118(24): 5519-5525.

Crews, L., Masliah, E. (2010). Molecular mechanisms of neurodegeneration in Alzheimer's disease. *Human Molecular Genetics*, 19(R1): R12-R20.

Crowther, D.C., Kinghorn, K.J., Miranda, E., Page, R., Curry, J.A., Duthie, F.A.I., Gubb, D.C., Lomas, D.A. (2005). Intraneuronal Aβ, non-amyloid aggregates and neurodegeneration in a *Drosophila* model of Alzheimer's disease. *Neuroscience*, 132(1): 123-135.

Fisher, A.B. (2011). Peroxiredoxin 6: A Bifunctional Enzyme with Glutathione Peroxidase and Phospholipase A_2 Activities. *Antioxidants & Redox Signaling*, 15(3): 831-844.

Hansen, D.V., Hanson, J.E., Sheng, M. (2018). Microglia in Alzheimer's disease. *Journal of Cell Biology*, 217(2): 459-472.

Iijima, K., Liu, H.-P., Chiang, A.-S., Hearn, S.A., Konsolaki, M., Zhong, Y. (2004). Dissecting the pathological effects of human Aβ40 and Aβ42 in *Drosophila*: A potential model for Alzheimer's disease. *PNAS*, 101(17): 6623-6628.

Iijima-Ando, K., Iijima, K. (2010). Transgenic *Drosophila* models of Alzheimer's disease and tauopathies. *Brain Structure and Function*, 214(2): 245-262.

Jeibmann, A., and Paulus, W. (2009). *Drosophila melanogaster* as a Model Organism of Brain Diseases. *International Journal of Molecular Sciences*, 10(20): 407-440.

Jensen, K.T., Fløe, L., Petersen, T.S., Huang, J., Xu, F., Bolund, L., Luo, Y., Lin, L. (2017). Chromatin accessibility and guide sequence secondary structure affect CRISPR-Cas9 gene editing efficiency. *FEBS Letters*, 591(13): 1892-1901.

Kanai, S., Ishihara, K., Kawashita, E., Tomoo, T., Nagahira, K., Hayashi, Y., Akiba, S. (2016). ASB14780, an Orally Active Inhibitor of Group IVA Phospholipase A_2, Is a Pharmacotherapeutic Candidate for Nonalcoholic Fatty Liver Disease. *The Journal of Pharmacology and Experimental Therapeutics*, 356(3): 604-614.

Kim, K.H., Lee, W., Kim, E.E. (2016). Crystal structures of human peroxiredoxin 6 in different oxidation states. *Biochemical and Biophysical Research Communications*, 477(4): 717-722.

Lee, I., Dodia, C., Chatterjee, S., Feinstein, S.I., Fisher, A.B. (2014). Protection against LPS induced acute lung injury by a mechanism-based inhibitor of NADPH oxidase (type 2). *AJP LUNG*, 306(7): L635-L644.

Lee, S.L., Carthew, R.W. (2003). Making a better RNAi vector for *Drosophila*: use of intron spacers. *Methods*, 30(4): 322-329.

Miquel, J., Lundgren, P.R., Bensch, K.G., Atlan, H. (1976). Effects of temperature on the life span, vitality and fine structure of Drosophila melanogaster. *Mechanisms of ageing and development*, 5(5): 347-370.

Murakami, M., Kudo, I. (2002). Phospholipase A2. *The Journal of Biochemistry*, 131(3): 285-292.

Nilsberth, C., Westlind-Danielsson, A., Eckman, C.B., Condron, M.M., Axelman, K., Forsell, C., Stenh, C., Luthman, J., Teplow, D.B., Younkin, S.G., Näslund, J., Lannfelt, L. (2001). The 'Arctic' APP mutation (E693G) causes Alzheimer's disease by enhanced protofibril formation. *Nature Neuroscience*, 4(9): 887-893.

Ong, W.-Y., Farooqui, T., Kokotos, G., Farooqui, A.A. (2015). Synthetic and Natural Inhibitors of Phospholipase A_2: Their Importance for Understanding and Treatment of Neurological Disorders. *ACS Chemical Neuroscience*, 6(6): 814-831.

Port, F., Muschalik, N., Bullock, S. (2015). CRISPR with independent transgenes is a safe and robust alternative to autonomous gene drives in basic research. *bioRxiv*.

Power, J.H.T., Asad, S., Chataway, T.K., Chegini, F., Manavis, J., Temlett, J.A., Jensen, P.H., Blumbergs, P.C., Gai, W.-P. (2008). Peroxiredoxin 6 in human brain: molecular forms, cellular distribution and association with Alzheimer's disease pathology. *Acta Neuropathologica*, 115(6): 611-622.

Querfurth, H.W., LaFerla, F.M. (2010). Mechanisms of Disease: Alzheimer's Disease. *The New England Journal of Medicine*, 362(4): 329-344.

Shaukat, Z., Liu, D., Gregory, S. (2015). Sterile Inflammation in *Drosophila*. *Mediators of Inflammation*.

Thomas, M.H., Pelleieux, S., Vitale, N., Olivier, J.L. (2016). Dietary arachidonic acid as a risk factor for age-associated neurodegenerative diseases: Potential mechanisms. *Biochemie*, 130: 168-177.

Tomoo, T., Nakatsuka, T., Katayama, T., Hayashi, Y., Fujieda, Y., Terakawa, M., Nagahira, K. (2014). Design, Synthesis, and Biological Evaluation of 3-(1-Aryl-1*H*-indol-5-yl)propanoic Acids as New Indole-Based Cytosolic Phospholipase $A_2\alpha$ Inhibitors. *Journal of Medicinal Chemistry*, 57(17): 7244-7262.

Vázquez-Medina, J.P., Tao, J.-Q., Patel, P., Bannitz-Fernandez, R., Dodia, C., Sorokina, E.M., Feinstein, S.I., Chatterjee, S., Fisher, A.B. (2019). Genetic inactivation of the phospholipase A_2 activity of peroxiredoxin 6 in mice protects against LPS-induced acute lung injury. *AJP LUNG*, 316(4): L656-L668.

Yanes, O., Clark, J., Wong, D.M., Patti, G.J., Sánchez-Ruiz, A., Benton, H.P., Trauger, S.A., Desponts, C., Ding, S., Siuzdak, G. (2010). Metabolic oxidation regulates embryonic stem cell differentiation. *Nature Chemical Biology*, 6(6): 411-417.

Yun, H.-M., Jin, P., Han, J.-Y., Lee, M.-S., Han, S.-B., Oh, K.-W., Hong, S.-H., Jung, E.-Y., Hong, J.T. (2013). Acceleration of the Development of Alzheimer's Disease in Amyloid Beta-Infused Peroxiredoxin 6 Overexpression Transgenic Mice. *Molecular Neurobiology*, 48(3): 941-951.

Zhang, S.L., Zhifeng, Y., Arnold, D.M., Artiushin, G., Sehgal, A. (2018). A Circadian Clock in the Blood-Brain Barrier Regulates Xenobiotic Efflux. *Cell*, 173(1): 130-139